

Multiphase groundwater flow near cooling plutons

Daniel O. Hayba

U.S. Geological Survey, Reston, Virginia

Steven E. Ingebritsen

U.S. Geological Survey, Menlo Park, California

Abstract. We investigate groundwater flow near cooling plutons with a computer program that can model multiphase flow, temperatures up to 1200°C, thermal pressurization, and temperature-dependent rock properties. A series of experiments examines the effects of host-rock permeability, size and depth of pluton emplacement, single versus multiple intrusions, the influence of a caprock, and the impact of topographically driven groundwater flow. We also reproduce and evaluate some of the pioneering numerical experiments on flow around plutons. Host-rock permeability is the principal factor influencing fluid circulation and heat transfer in hydrothermal systems. The hottest and most steam-rich systems develop where permeability is of the order of 10^{-15} m². Temperatures and life spans of systems decrease with increasing permeability. Conduction-dominated systems, in which permeabilities are $\leq 10^{-16}$ m², persist longer but exhibit relatively modest increases in near-surface temperatures relative to ambient conditions. Pluton size, emplacement depth, and initial thermal conditions have less influence on hydrothermal circulation patterns but affect the extent of boiling and duration of hydrothermal systems. Topographically driven groundwater flow can significantly alter hydrothermal circulation; however, a low-permeability caprock effectively decouples the topographically and density-driven systems and stabilizes the mixing interface between them thereby defining a likely ore-forming environment.

Introduction

Twenty years ago classic papers by *Norton and Knight* [1977] and *Cathles* [1977] examined density-driven groundwater flow caused by a cooling pluton. These papers have greatly influenced our thinking about magmatic-hydrothermal systems and are still commonly cited in the hydrothermal literature. These were truly pioneering works because they employed sophisticated numerical flow and heat transport models at a time when transport modeling was rare, even in the context of low-temperature groundwater systems.

The numerical models used for this first-generation work had limitations, necessitated primarily by the less powerful computers available 20 years ago. For example, *Norton and Knight* [1977] and *Cathles* [1977] applied the "Boussinesq approximation," which assumes that fluid density is constant except in the buoyancy-force term. There was thus no allowance for flow due to in situ changes in fluid density, so their simulations could not include the effects of thermal pressurization. In fact, fluid pressure was not calculated directly because each of their numerical models solved governing equations in which the independent variables were temperature and stream function. Their stream function approach also did not produce truly transient results because each time step required a

steady state solution (see discussions by *Furlong et al.* [1991, p. 472], *Evans and Raffensperger* [1992], and *Hanson* [1992]). The early models were also limited to single-phase conditions: *Norton and Knight* [1977] avoided the two-phase region, and *Cathles* [1977] assumed that the fluid in each finite difference block was either all steam or all liquid. Other simplifying assumptions involved the permeability of pluton; *Cathles* [1977] assigned identical, nonvarying values to the host rock and pluton, whereas *Norton and Knight* [1977] generally made the pluton relatively impermeable. Neither study considered the competing influence of topographically driven flow.

Many of the limitations of these earliest models of groundwater flow near cooling plutons have since been addressed. Norton and others clearly realized the importance of thermal pressurization and quantified this process in a series of papers [e.g., *Knapp and Knight*, 1977; *Norton*, 1990; *Dutrow and Norton*, 1995]; work by *Delaney* [1982], *Sammel et al.* [1988], and *Hanson* [1992] has also contributed to our understanding of this effect. Other studies have considered heterogeneous permeabilities [e.g., *Parmentier*, 1981; *Gerdes et al.*, 1995] or time (temperature)-dependent permeabilities [e.g., *Norton and Taylor*, 1979; *Dutrow and Norton*, 1995] and the influence of topography [*Sammel et al.*, 1988; *Birch*, 1989; *Hanson*, 1996].

The novel aspect of the work presented here is the more realistic treatment of two-phase (steam-liquid) flow and its consequences. We present the results of some simple, generic cooling-pluton experiments that extend the pioneering work of *Norton and Knight* [1977] and *Cathles*

This paper is not subject to U.S. copyright. Published in 1997 by the American Geophysical Union.

Paper number 97JB00552.

[1977]. Our numerical models utilized the HYDROTHERM computer program [Hayba and Ingebritsen, 1994] that simulates the transient flow of water at temperatures up to 1200°C and pressures up to 1000 MPa, includes such processes as thermal pressurization and multiphase flow, and allows permeabilities to vary as functions of temperature. Although this program can more accurately represent fluid flow driven by cooling plutons than the early models, our simulations still incorporate numerous simplifying assumptions; the most significant of these are that the fluid is pure water and that there is no contribution from magmatic fluids. Our results demonstrate how groundwater flow in magmatic-hydrothermal systems varies because of the effects of host-rock permeability, the presence of a caprock, size of the pluton, depth of emplacement, single versus multiple intrusions, and the influence of topography. In the appendix, we reevaluate some of the original models run by Norton and Knight [1977] and Cathles [1977].

Mathematical Approach

As recently a few years ago, there were no fluid-flow simulation codes that described the physical properties of water over the pressure-temperature range relevant to magmatic-hydrothermal systems. Existing codes were limited to simulating either (1) single-phase flow, like those used by Norton and Knight [1977] and Cathles [1977] or (2) two-phase systems at subcritical temperatures, like the simulators used by geothermal reservoir engineers [e.g., Pruess, 1991]. Today, there are at least three multiphase, high-temperature codes, including the U.S. Geological Survey's (USGS) HYDROTHERM [Hayba and Ingebritsen, 1994]. The simulations presented here used version 2.0 of that code; version 2.1 is available from the USGS via the World Wide Web at <http://water.usgs.gov/software/> in the groundwater section and via anonymous ftp from [water.usgs.gov \(/pub/software\)](http://water.usgs.gov/pub/software/).

HYDROTHERM uses a finite difference approach to simulate multiphase flow of pure water and heat at temperatures between 0°-1200°C and pressures between 0.05-1000 MPa. It solves the following expressions for mass and energy conservation:

$$\begin{aligned} \partial[n S_w \rho_w + n S_s \rho_s] / \partial t - \nabla \cdot [k k_{rs} \rho_s / \mu_s \cdot (\nabla P - \rho_s g \nabla D)] \\ - \nabla \cdot [k k_{rw} \rho_w / \mu_w \cdot (\nabla P - \rho_w g \nabla D)] - R_m = 0 \end{aligned} \quad (1)$$

$$\begin{aligned} \partial[n S_w \rho_w H_w + n S_s \rho_s H_s + (1-n) \rho_R H_R] / \partial t \\ - \nabla \cdot [k k_{rs} \rho_s H_s / \mu_s \cdot (\nabla P - \rho_s g \nabla D)] \\ - \nabla \cdot [k k_{rw} \rho_w H_w / \mu_w \cdot (\nabla P - \rho_w g \nabla D)] \\ - \nabla \cdot (K_m \nabla T) - R_H = 0 \end{aligned} \quad (2)$$

respectively, where n is porosity, S is volumetric saturation ($S_w + S_s = 1$), ρ is density, t is time, k is intrinsic permeability, k_r is relative permeability ($0 \leq k_r \leq 1$), μ is dynamic viscosity, P is pressure, g is gravitational acceleration, D is depth, H is enthalpy, K_m is medium thermal conductivity, T is temperature, R_m and R_H are mass and energy source/sink flow rate terms, respectively, and the subscripts w , s , and R refer to liquid water, steam, and rock (matrix), respectively. The dependent variables in (1) and (2) are the pressure and enthalpy of the fluid in place. Unlike pressure and temperature, using pressure and enthalpy as the dependent

variables uniquely specifies the thermodynamic state of the fluid under both single- and two-phase conditions. For two-phase conditions within a single finite difference block, the enthalpy of the fluid in place H_f is defined by

$$H_f = [H_w S_w \rho_w + H_s S_s \rho_s] / [S_w \rho_w + S_s \rho_s] \quad (3)$$

Equations (1) and (2) are strongly coupled and highly nonlinear, because a number of the independent variables are functions of the dependent variables P and H . HYDROTHERM uses Newton-Raphson iteration to treat the nonlinear coefficients. Mass and energy balances for each finite difference block determine convergence.

Assumptions implicit in these equations are that a two-phase form of Darcy's Law is valid; that rock and water are in local thermal equilibrium; and that capillary-pressure effects, compressible work, and heat transfer by dispersion are negligible. Several constitutive relations complete the description of the system [Faust and Mercer, 1977, 1979; Hayba and Ingebritsen, 1994]. In this study, linear functions describe relative permeabilities with residual liquid and steam saturations of 0.3 and 0.0, respectively (that is, liquid becomes immobile at a steam saturation of 0.7). A large (2 Mbyte) lookup table interrogated by a bicubic spline routine provides fluid densities, viscosities, and temperatures. We use fluid density and temperature values from the routines of Haar et al. [1984] and viscosity values from the formulation by Sengers and Watson [1986]. Cubic splines describe fluid properties at saturation.

Each of the thermodynamic variables in (1) and (2) is finite at the critical point ($P = 22.055$ MPa, $H = 2086.0$ kJ/kg, $T = 373.98^\circ\text{C}$, $\rho = 322$ kg/m³, and $\mu = 3.94 \times 10^{-5}$ Pa s). Above the critical point, the distinction between liquid and steam disappears, and the values assigned to the saturation variables become arbitrary. For computational purposes, we treat supercritical blocks as though they contain two phases with identical properties and gradually decrease the saturation from 1 (liquid) to 0 (steam) radially about the critical point. This technique helps to better estimate the average fluid properties for flow between supercritical blocks adjacent to single-phase, subcritical blocks thereby avoiding oscillation problems. With the P - H formulation, near-critical computations [e.g., Ingebritsen and Hayba, 1994] have actually proven to be less difficult than problems involving lower-pressure phase transitions, where there is a larger contrast in fluid properties.

Boundary and Initial Conditions

In most of our simulations, we used a 10 km wide by 4 km deep planar (two-dimensional) model and a 2 km tall pluton with a half width of 0.5 km (Figure 1). The model has a nominal thickness of 1 m. The pluton is emplaced at a depth of 2 km for flat topography and at shallower levels when the overlying topographic slope is 20%. A few simulations involve 2 km by 2 km (half width) plutons emplaced at a depth of 5 km. Some models include a 250 m thick by 0.6 km long, low-permeability horizon which represents a caprock overlying the hydrothermal system. Grid spacing is approximately 100 m (X) by 250 m (Z) near the pluton, becoming coarser in X with distance from the pluton.

The upper boundary of the model represents the water table, with fluid pressure and temperature held constant at

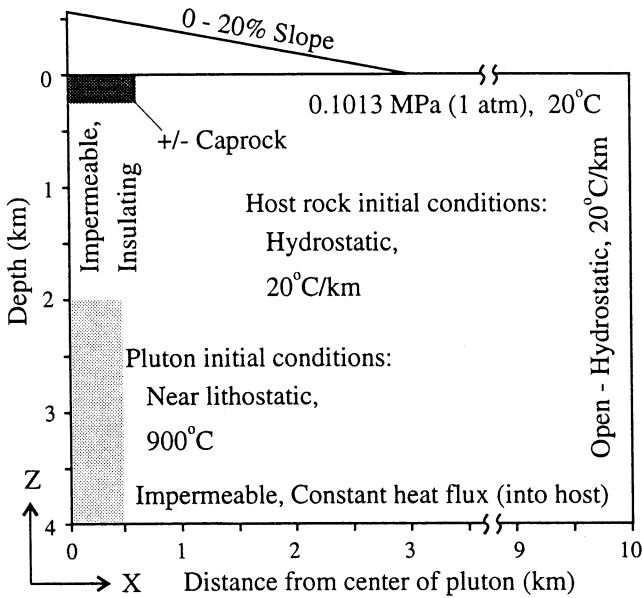


Figure 1. Geometric model showing boundary and initial conditions for the simulations presented in Figures 3 - 7, 12a and 12b, and 13. Simulations with different geometries and (or) initial condition are so noted.

0.1013 MPa (1 atm) and 20°C. The bottom is impermeable, with a constant basal heat flux of 63 mW/m² (~1.5 HFU) into the host rock and no basal heat flux into the pluton. The left-hand boundary represents a plane of symmetry and is thus impermeable and insulating. The right-hand boundary, which is located sufficiently far from the pluton so as to have little impact on the simulations, is an open boundary at hydrostatic pressures and a temperature gradient of 20°C/km.

A constant pressure-temperature or “free” upper boundary condition is frequently applied in studies of subsea fluid circulation and regional groundwater flow. It effectively represents an infinite source or sink of fluid, donating or accepting fluid according to the hydraulic gradients in the underlying system. This construct is eminently reasonable in the seafloor context. In most cases, it is also a reasonable representation of the water table in a continental environment, but in this context the actual fluid source (meteoric recharge) is finite. In our simulations, the maximum simulated downflow (recharge) rate is permeability-dependent and reaches as much as 0.5 m/yr for flat topography with host-rock permeabilities of 10^{-13.5} m². Simulations with topographic slopes of 20% and permeabilities of 10⁻¹⁵ m² led to recharge rates of less than 0.2 m/yr. These values are reasonable in light of published recharge estimates for volcanic highlands that range up to 1 m/yr in the Cascade Range [Ingebritsen et al., 1994] and 4 m/yr on Hawaii [Takasaki, 1993], suggesting that a free upper boundary is appropriate for these experiments.

The initial conditions within the host rock are usually a 20°C/km temperature gradient and a hydrostatic pressure gradient, although the initial conditions for some simulations reflect the effects of earlier intrusions. Each simulation begins with the instantaneous intrusion of a 900°C pluton. We also specify that initial pressures within the pluton are approximately 10% less than lithostatic pressures.

Table 1. Rock Properties

Property	Pluton	Host	Caprock
Permeability - isotropic, m ²	f(T)	f(T)	10 ⁻¹⁸
Porosity, %	5	10	5
Heat capacity, J/(kg K)	f(T)	1000	1000
Thermal conductivity, W/(m K)	2	2	2
Rock density, kg/m ³	2500	2500	2500

See also Figure 2.

Intrinsic permeability and rock heat capacity vary as functions of temperature, whereas other rock properties (porosity, density, and heat capacity) are constant throughout the simulations (Table 1). At temperatures above 500°C (Figure 2), we assume that the permeability of the pluton is negligibly low (10⁻²² m²). As temperature decreases from 500° to 400°C, permeability increases log linearly to 10⁻¹⁷ m². As temperature decreases further to 360°C, we assume that the intrusion becomes brittle, that fractures develop, and that the pluton becomes as permeable as the surrounding host rock (we consider host-rock permeabilities of 10⁻¹⁷-10^{-13.5} m²). Treating the permeability of the pluton as a function of temperature approximates the effect of the brittle/ductile transition at about 360°C [Fournier, 1991], allowing the hydrothermal system to mine heat from the intrusion as fractures develop in the caprock. The temperature-dependent permeability function also mitigates one of the major effects of our pure-water assumption. Adding other components to the H₂O system greatly expands the two-phase region [e.g., Fournier, 1987]. In particular, with the addition of salt, two fluid phases will exist at temperatures above the pure-water critical point [e.g., Bischoff and Pitzer, 1989]. Although the HYDROTHERM equations of state cannot model the difference in fluid properties caused by this “supercritical phase separation,” its effect on advective heat transport is minimized by the low permeability at supercritical temperatures (Figure 2).

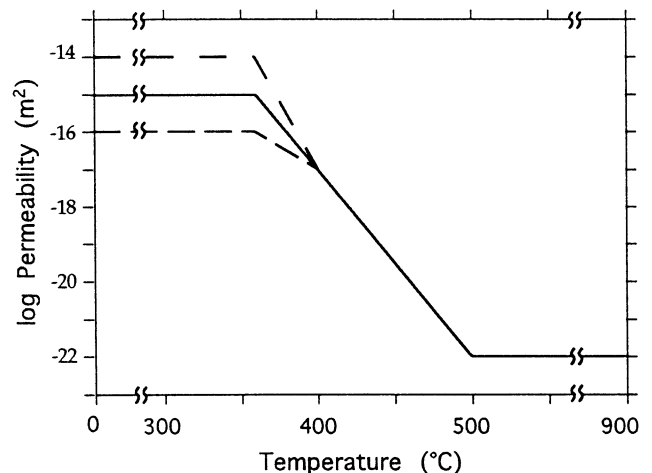


Figure 2. Plot showing the permeability-temperature relation used to approximate the effect of a brittle/ductile transition at about 360°C

We apply the same temperature-dependent function to the host-rock permeability, but the effect is generally insignificant. For permeabilities greater than 10^{-16} m², host rocks adjacent to the pluton rarely exceed 360°C because heat transfer is dominated by advection. Exceptions occur in simulations where the initial conditions represent the effects of an earlier intrusion; in these instances, host-rock temperatures near the pluton reach 500°C, causing significant local decreases in permeability. In this study, we do not consider any anisotropy in permeability ($k_x=k_z$), and the only heterogeneity in permeability considered (other than that of the temperature-dependent function) is the inclusion of a caprock in some experiments.

Rock heat capacity also varies as a function of temperature to account for the latent heat of crystallization. We follow *Hanson and Barton's* [1989] approach, doubling the heat capacity of the pluton (2000 J/(kg K)) for temperatures between 900° and 750°C. This approach treats heat release by crystallization as a continuous process over a finite temperature interval and yields more accurate temperature estimates close to the intrusion than does artificially increasing the intrusion temperature.

The dimensions, depth of emplacement, and initial temperature of the simulated intrusion are appropriate to a granitic pluton, rather than a basalt. This may be true of the temperature-dependent permeability function as well, although data bearing on this point are limited. Basalt has higher inherent strength than granite, and evidence from Skaergaard [*Manning and Bird*, 1991] and the mid-ocean-ridge environment [*Brikowski and Norton*, 1989] suggests that in basaltic terrane secondary porosity can be generated at relatively high temperatures. Further, there is strong geochemical evidence for supercritical phase separation in some seafloor hydrothermal systems [e.g., *Lowell et al.*, 1995] and for meteoric hydrothermal alteration of gabbroic plutons at very high temperatures [e.g., *Taylor*, 1990]. However, *Fournier* [1991] argues for low permeabilities at temperatures >370°-400°C at the Nesjavellir, Iceland, geothermal field, consistent with observations at other, nonbasaltic fields. The apparent disagreement about temperature-permeability relations in the literature may have to do with the definition of "low" permeability. For example, host-rock permeability may be low enough to preclude advective heat transport and (or) to permit hydraulic fracturing yet may be "high" enough to allow significant advective solute transport.

Influence of Permeability

In this section, we illustrate how flow systems driven by cooling plutons vary as a function of host-rock permeability. In these simulations, a 2 x 1 km pluton intrudes initially cool host rocks at a depth of 2 km. In hydrothermal and metamorphic systems, host-rock permeabilities may range from less than 10^{-19} m² in areas of contact metamorphism to values exceeding 10^{-12} m² in mid-oceanic-ridge hydrothermal systems (data summarized by *Hanson* [1995]). We considered permeabilities ranging from 10^{-18} m² to $10^{-13.5}$ m², because this range effectively spans the transition from conduction-dominated heat transfer to advection-dominated heat transfer.

Figure 3 shows the evolving temperature and fluid-flow patterns near intrusions hosted by relatively impermeable ($k \leq 10^{-16}$ m²) rocks, such that the dominant heat-transport

mechanism is conduction. Immediately following emplacement, thermal pressurization dominates flow, driving fluids away from the pluton. The importance and duration of thermal pressurization as a driving force for flow varies inversely with the permeability of the host rocks and directly with porosity and the temperature contrast between the pluton and its host [*Delaney*, 1982]. At host-rock permeabilities of 10^{-16} m², thermal pressurization is a significant force driving flow for only the first few hundred years following an intrusion into porous ($n = 0.10$) country rocks that are initially cool. For host-rock permeabilities of 10^{-17} m², thermal pressurization is the dominant driving force for several thousand years (Figure 3a). For even less permeable ($k \leq 10^{-18}$ m²), but still porous (0.10) host rocks, simulated early-time pressures near the magma exceed lithostatic. However, porosity strongly affects thermal pressurization [*Delaney*, 1982; *Hanson*, 1995], and in simulations using the same permeability (10^{-18} m²) but considerably lower porosity (0.001), pressures increase only to somewhat above hydrostatic. Recently, *Hanson* [1992, 1995] critically examined fluid migration in very low-permeability ($k \leq 10^{-18}$ m²), low-porosity ($n = 0.001$) hosts and demonstrated that fluid production from the magma and from the wall rocks are more important processes than thermal pressurization in elevating fluid pressure near the pluton. Our work focuses on flow in more permeable and porous hosts.

Following the initial period of flow dominated by thermal pressurization, a sluggish, density-driven convection system develops (Figures 3b and 3d). For permeabilities of 10^{-17} m², maximum fluid-particle velocities decrease from about 0.3 m/yr at 5000 years to about 0.04 m/yr at 30,000 years. Velocities are roughly an order of magnitude larger for permeabilities of 10^{-16} m². For both cases, advective heat transport is minor, and the evolving thermal regimes are very similar (compare Figures 3a-3c with Figures 3d-3f). Because conduction dominates heat transfer, temperatures at shallow depths remain well below the boiling-point-depth curve, and near-surface temperatures and heat flow reach their maxima at approximately 30,000 years. Slight differences in the pressure regimes for the two systems influence whether a boiling zone develops nearer the pluton. At host permeabilities of 10^{-16} m², a small zone of superheated steam (usually grading upward into a steam/water mixture) forms directly above the pluton during the first 5000 years following emplacement. At lower permeabilities, pressures in this region are sufficiently high to preclude boiling, and a supercritical fluid directly above the pluton gives way to compressed water at shallower levels.

For host-rock permeabilities of 10^{-15} m² or greater (Figure 4), the hydrothermal system surrounding a cooling pluton is dramatically different from the conduction-dominated case (Figure 3). The dominant heat-transfer mechanism is advection, and the hydrothermal systems wax and wane much more rapidly, attaining maximum near-surface temperatures within 2000 to 6000 years following emplacement. Thus, depending upon permeability, the effective life span of a system driven by a single 2 x 1 km pluton can range from about 30,000 years to less than 10,000 years.

In hydrothermal systems hosted by rocks with permeabilities of 10^{-15} m², boiling zones and temperature-depth profiles change markedly as the system evolves. Shortly

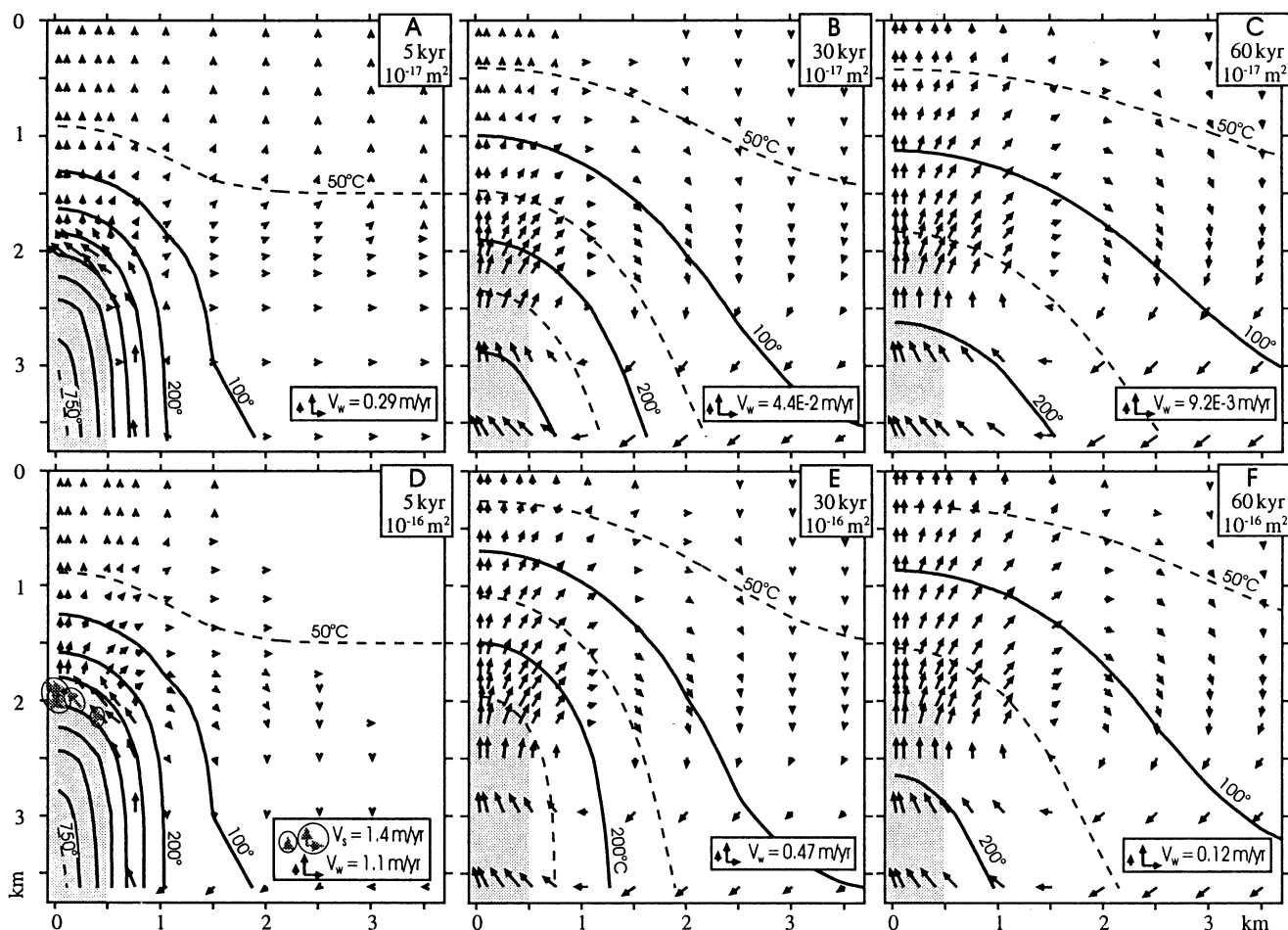


Figure 3. Simulation results for host rocks with low permeabilities (10^{-17} – 10^{-16} m^2) showing temperature contours and fluid-flow vectors at selected times. Solid arrows represent flow vectors for liquid and supercritical water. Shaded arrows with enclosing circles show steam velocities and thus indicate boiling. Flow vectors are scaled logarithmically over 2 orders of magnitude relative to the maximum fluid-particle velocities V_w (water) and V_s (steam); the smaller, vertical vector in the scale shows fluid velocity at 1 order of magnitude lower than the maximum vector scale. (a)–(c) Permeability = 10^{-17} m^2 . (d)–(f) Permeability = 10^{-16} m^2 . Note at temperatures greater than 360°C, permeabilities decrease with increasing temperatures (see Figure 2).

following an intrusion, a small two-phase zone, grading downward into superheated steam, develops directly above the pluton, persisting for about 5000 years (Figures 4a and 5). This deep boiling zone is similar to the one described above for host permeabilities of 10^{-16} m^2 . As the pluton cools, the boiling zone retreats toward greater depths (see Figure 5: 2500 versus 5000 years). Depending upon the conditions in the overlying water column, pressures at depths greater than approximately 2.2 km exceed the critical pressure and thus preclude boiling near the pluton. As the deep boiling subsides, the upwelling plume begins to boil at shallower depths, and for a short time (at about 6250 years), two-phase conditions extend from the surface to depths of greater than 1.5 km (Figures 4b and 5b). The volumetric proportion of steam in the pore space reaches a maximum of about 40% at a depth of 250 m. Advective heat transport is not sufficient to maintain boiling conditions to depths greater than 1.5 km for long, and the boiling zone gradually shrinks toward the surface (Figures 4c and 5). Shallow two-phase conditions persist for about 7000 years (from about 6000 to 13,000 years). The

temperature-depth profiles shown in Figure 5a also illustrate the thermal evolution of the system. Initially, there is a steep temperature gradient directly above the pluton. Gradually, the steepest part of the thermal gradient migrates toward shallower levels. At 7500 years, the steepest gradient occurs near the surface, and temperatures follow the boiling-point-depth curve to depths of about a kilometer. The system begins to wane by 15,000 years, and temperatures actually decrease with depth; the hottest fluids in the system occur at a depth of approximately 500 m. Here the temperature reversal results from transient effects in a homogeneous system, rather than confined lateral flow, as is often assumed when similar temperature profiles are measured in the field.

Where a pluton intrudes highly permeable (10^{-14} m^2) host rocks, fluid migration is rapid (Figures 4d–4f), and great volumes of fluid quickly sweep heat away from the pluton. The maximum temperature of the upwelling plume is 50°–100°C lower than in the case with host-rock permeabilities of 10^{-15} m^2 . The only steam that evolves in these more permeable systems is a minor amount near the surface (e.g.,

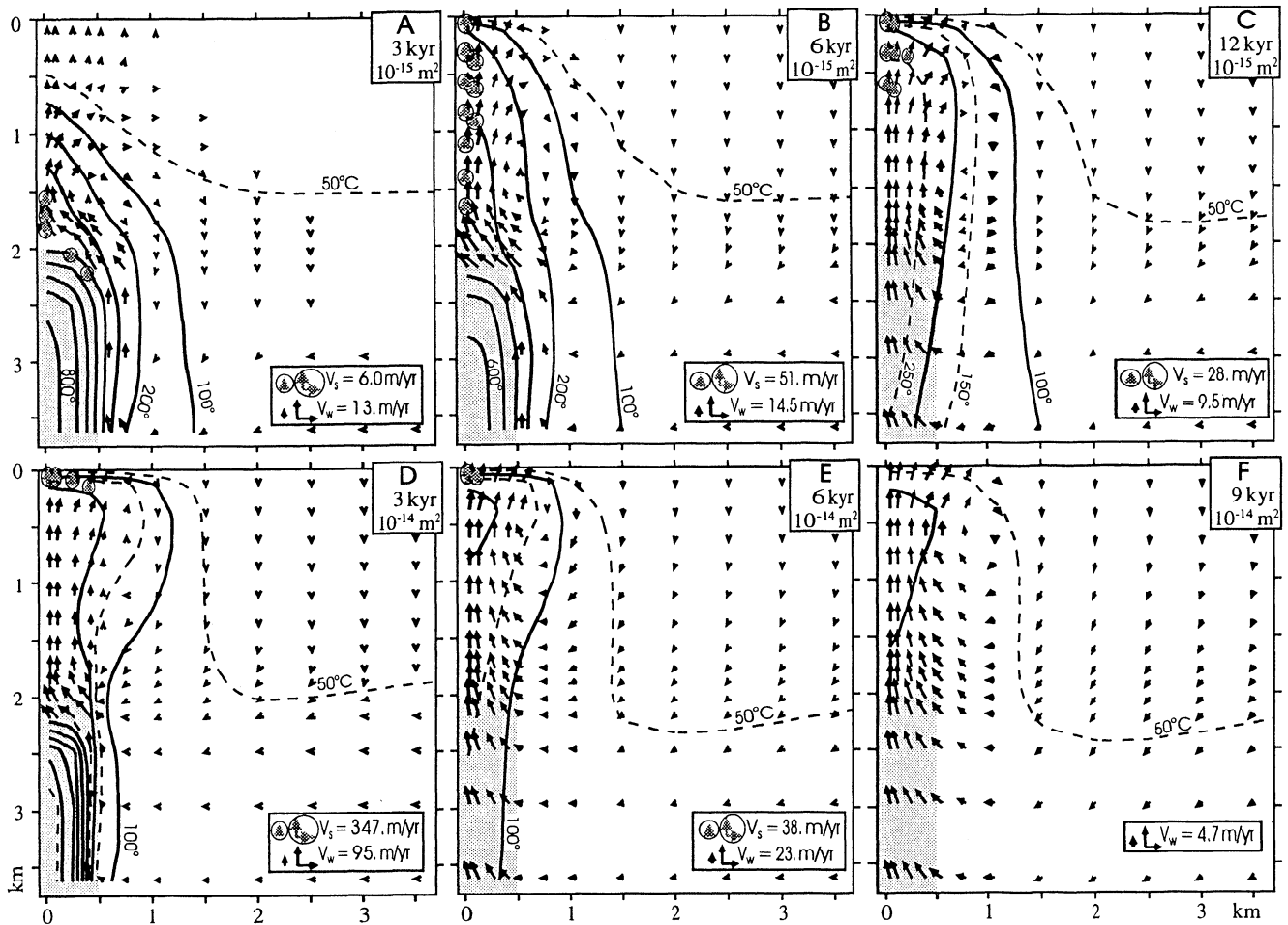


Figure 4. Simulation results for host rocks with high permeabilities (10^{-15} - 10^{-14} m^2) showing temperature contours and fluid-flow vectors at selected times. Flow vectors are as described for Figure 3. (a)-(c) Permeability = 10^{-15} m^2 . (d)-(f) Permeability = 10^{-14} m^2 . Note at temperatures greater than 360°C , permeabilities decrease with increasing temperatures (see Figure 2).

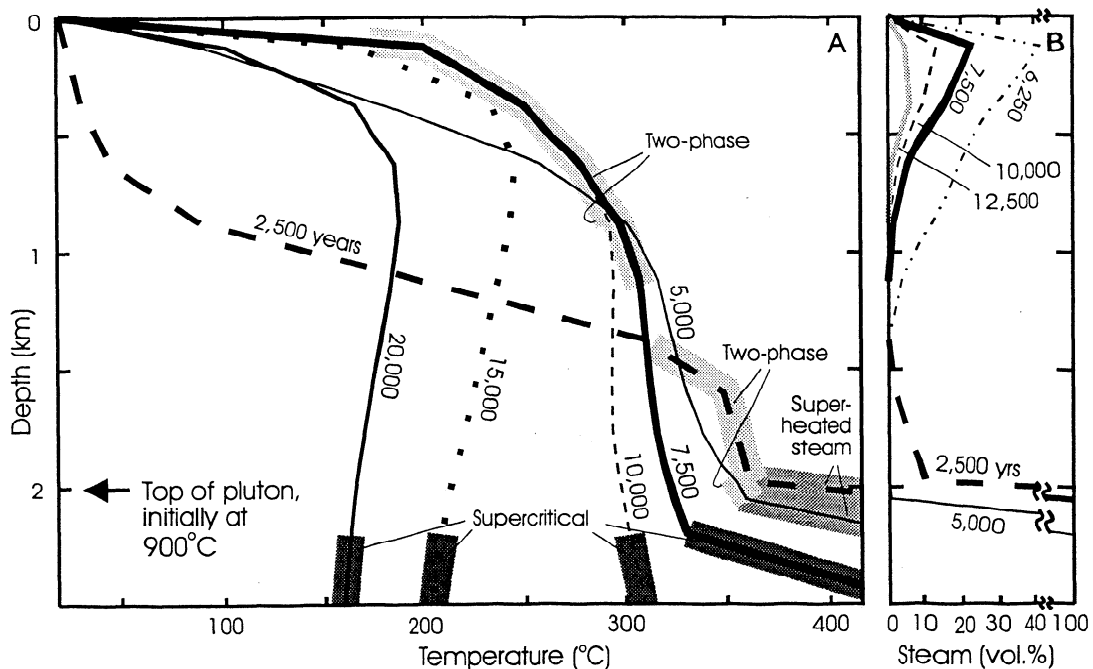


Figure 5. (a) Temperature-depth profiles above the center of the pluton (along left side of model) at selected times for a host-rock permeability of 10^{-15} m^2 . (b) Profiles showing volumetric proportion of steam at the same location and times.

Figure 4d). Deep-seated boiling directly above the pluton does not occur.

The simulations shown in Figures 3 and 4 demonstrate the controlling influence of host-rock permeability on the maximum temperature, the amount of steam, and the duration of hydrothermal systems. Figure 6 helps summarize the effects of permeability by showing temperature histories for different permeabilities at three selected depths. The hottest hydrothermal systems at shallow depths (< 1.5 km, Figures 6a and 6b) develop where host-rock permeability is of the order of 10^{-15} m^2 . Boiling conditions persist in these systems for thousands of years, and temperatures at < 1 km exceed 200°C for nearly 20,000 years. Systems with permeabilities of 10^{-16} m^2 or less are conduction-dominated. In these systems, temperatures near the pluton are elevated for more than 50,000 years

(Figure 6c), but near-surface temperatures increase only slightly over this time frame (Figure 6a). Systems with permeabilities greater than 10^{-15} m^2 are increasingly cooler and shorter-lived (e.g., Figure 6b). Systems with permeabilities of 10^{-14} m^2 last for only about 5000 years, and boiling conditions develop only near the surface. Slightly more permeable ($10^{-13.5} \text{ m}^2$) systems last for less than 3500 years and do not appear to boil. This inverse relationship between permeability and temperature-duration reflects the fact that higher permeabilities allow greater volumes of water to rapidly advect heat away from the pluton. (Similar relations have been calculated for mid-ocean-ridge vents; see Lowell and Burnell [1991].)

The fluctuating temperatures evident in the higher-permeability ($\geq 10^{-14.5} \text{ m}^2$) simulations (Figure 6) are due to space discretization in the numerical model combined with

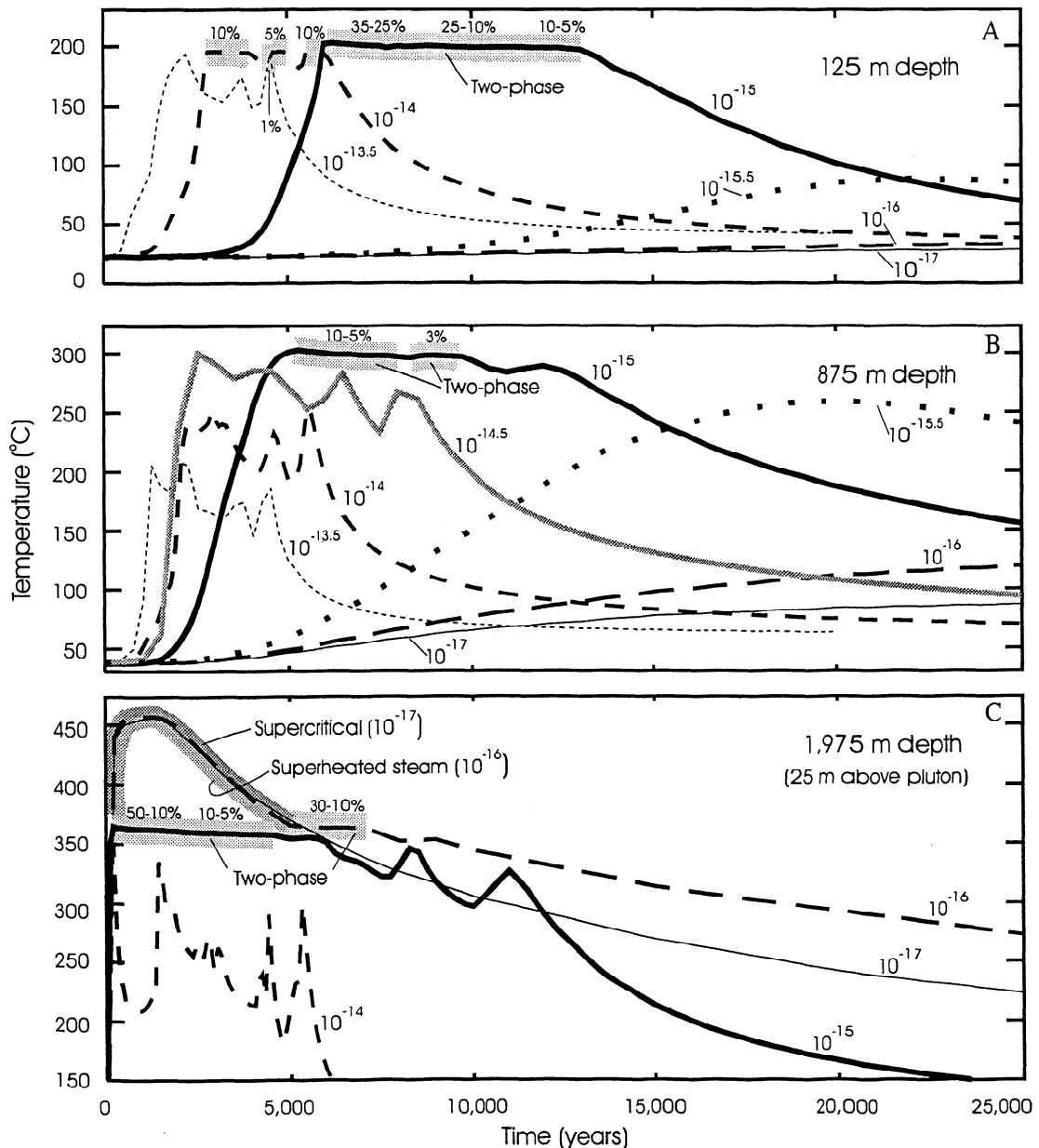


Figure 6. Temperature histories at selected depths above the center of the pluton (along left side of model) for various permeabilities: (a) 125 m, (b) 875 m, and (c) 1975 m. Pluton dimensions are 2 x 1 km intruded at 2 km depth in an initially cool environment. Volumetric vapor saturation is shown as a percentage.

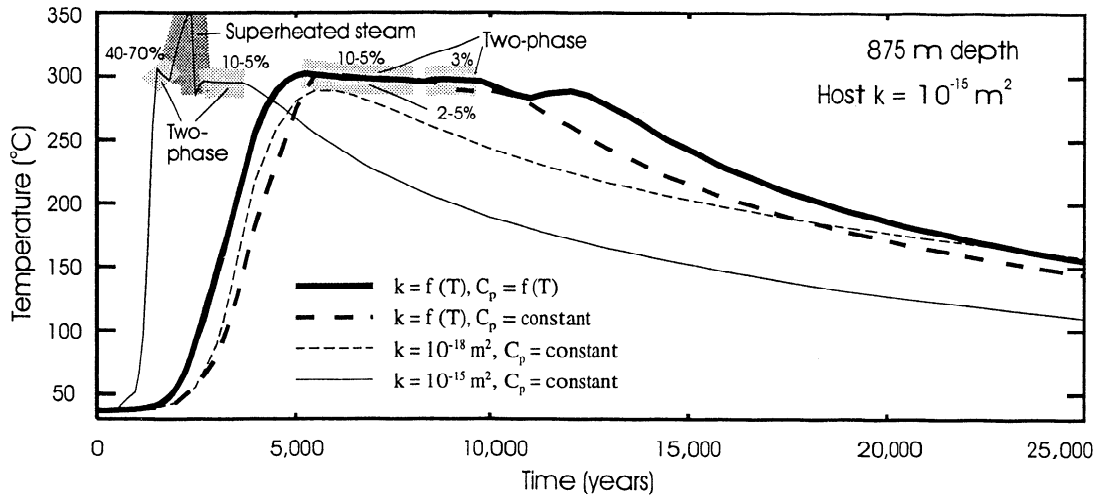


Figure 7. Temperature histories at 875 m depth above the center of the pluton (along left side of model) for different assumptions concerning the permeability and heat capacity (latent heat of crystallization) of the pluton. Constant heat capacity ignores heat of crystallization. Volumetric vapor saturation is shown as a percentage.

the temperature-dependent permeability function. As the temperature of a finite difference block in the pluton drops from 400° to 360°C, the permeability increases from a value of 10⁻¹⁷ m² to the value assigned to the surrounding host rock. For the higher permeability simulations, this increase is several orders of magnitude, which allows fluids to rapidly mine the heat from that block. We were able to verify that this thermal behavior is a discretization effect by (1) tracking and relating the temperature history of specific nodes within the pluton to thermal spikes in the shallower nodes and (2) refining the grid within the pluton to eliminate the spikes. Although these simulated temperature fluctuations are a numerical artifact, one can imagine analogous situations in nature when fractures open abruptly, exposing hot rock to large volumes of circulating fluids.

The results for these simulations are somewhat different if the heat capacity of the pluton and permeability are constants rather than temperature-dependent functions (Figure 7). As discussed previously, we account for the latent heat of crystallization by doubling the heat capacity of the pluton for temperatures ranging from 900° to 750°C. Ignoring this additional heat (but still treating permeability as a function of temperature) leads to hydrothermal systems that are slightly cooler, produce less steam, and have somewhat shorter life spans (bold dashed line). If the pluton also maintains its initially low permeability (10⁻¹⁸ m²) throughout its entire cooling history, the hydrothermal system is even cooler and generates no steam at a depth of 875 m (fine dashed line). This approach (which was used by Norton and Knight [1977]) predicts that moderately elevated temperatures of 100° to 150°C at about 1 km depth will persist for a longer time, because heat must transfer by conduction to the margins of the pluton before entering the hydrothermal system. If the permeability of the pluton is assumed to be identical to that of the host rock throughout its cooling history, the hydrothermal system transfers enough heat to produce superheated steam at depths of less than 1 km for a brief period but cools off quickly (fine line). This assumption (made by Cathles [1977] for a perme-

ability of 2.5 × 10⁻¹⁶ m²) generally seems inappropriate for permeabilities of 10⁻¹⁵ m² or greater because plastic deformation in the intrusion at temperatures above 400°C should greatly reduce permeability [Fournier, 1991], especially for granitic systems.

Results for the higher permeability systems ($k \geq 10^{-15} \text{ m}^2$, Figures 6a and 6b), where heat transfer is dominated by advection, indicate that the maximum temperature at any given depth within the upwelling plume decreases as permeability increases. Temperature and permeability data for various geothermal reservoirs [Björnsson and Bodvarsson, 1990] suggest a similar inverse relationship for natural systems (Figure 8, diamonds). Their data indicate that the highest-temperature (325°–350°C) geothermal reservoirs have permeabilities of about $3 \times 10^{-15} \text{ m}^2$ and that more permeable reservoirs tend to have lower maximum temperatures. For similar values of permeability, the measured temperatures of the natural systems slightly exceed the values predicted for the simulated systems (horizontal bars). We have no information about the depths at which

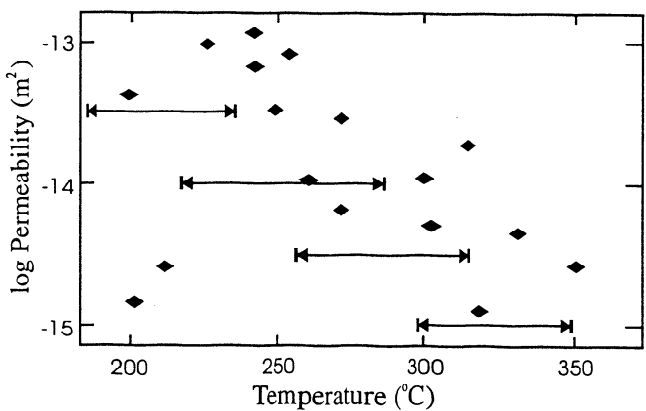


Figure 8. Permeability-temperature relations for various geothermal systems (diamonds, data from Björnsson and Bodvarsson [1990]) and simulated temperature ranges at 1600 m depth for various host-rock permeabilities (horizontal bars).

the observations were made, but boiling-point-with-depth relations [Haas, 1971] constrain depths to greater than about 1700 m at 330°C. In terms of permeability, the observed and simulated permeability-temperature relations appear to be offset by only about a half an order of magnitude. Because the details of the permeability measurements in the natural systems are unknown, rigorous comparison of the simulated and measured trends may not be warranted. However, we speculate that this difference may reflect the fact that the measured permeabilities are values for geothermal reservoirs, which are presumably the most permeable parts of larger hydrothermal systems.

Multiple Intrusions

The previous section showed how host-rock permeability influences hydrothermal circulation around a 2 x 1 km pluton intruded at a depth of 2 km into cool country rocks. Much of the heat provided by the pluton went to raising the temperature of host rocks initially at a normal geothermal gradient of 20°C/km. Those initial conditions represent an end-member of possible scenarios. In this section, we present some results from simulations in which a pluton intrudes host rocks that have been warmed, either conductively or advectively, by previous intrusions.

To represent a conductively preheated environment, we set initial conditions for pressure and enthalpy in the host rock that correspond to the 20,000 year solution for rocks with a permeability of 10^{-16} m^2 (similar to the 30,000 year solution shown in Figure 3e). After specifying a new host-rock permeability, each simulation then begins with the instantaneous intrusion of another pluton. Figure 9 shows

selected results for conductively preheated simulations for host-rock permeabilities ranging from 10^{16} to $10^{-13.5} \text{ m}^2$. The main differences between these results and those from the previous experiments with a cool host are the more rapid onset of maximum temperatures and the greater abundance of steam in the preheated case (compare Figures 6a and 6b with Figures 9a and 9b). The other notable difference is the increased temperature and steam saturation in the marginally permeable systems (i.e., permeabilities near the transition from conduction- to advection-dominated heat transport; $k = 10^{-16}$ to $10^{-15.5} \text{ m}^2$). At depths of about 1 km, the hottest conductively preheated system occurs at a relatively low permeability of $10^{-15.5} \text{ m}^2$.

In an advectively preheated environment (not shown), the timing of subsequent intrusions strongly influences the results because these systems heat and cool rapidly. For the size and depth parameters listed above and a host-rock permeability of 10^{-15} m^2 , a subsequent intrusion would have to follow the initial intrusion within about 20,000 years in order for the waning, earlier hydrothermal system to provide an appreciable increment of heat. More permeable systems have even shorter time frames (see Figure 7).

Influence of Depth of Emplacement

As the depth of emplacement increases, so does the volume of overlying rock that the pluton must heat in order to enhance near-surface temperatures. Consequently, deeper-based hydrothermal systems evolve more slowly and to somewhat lower temperatures than shallower-based systems. Figure 10 shows temperature histories at depths of 125 m and 875 m for intrusions with our familiar dimen-

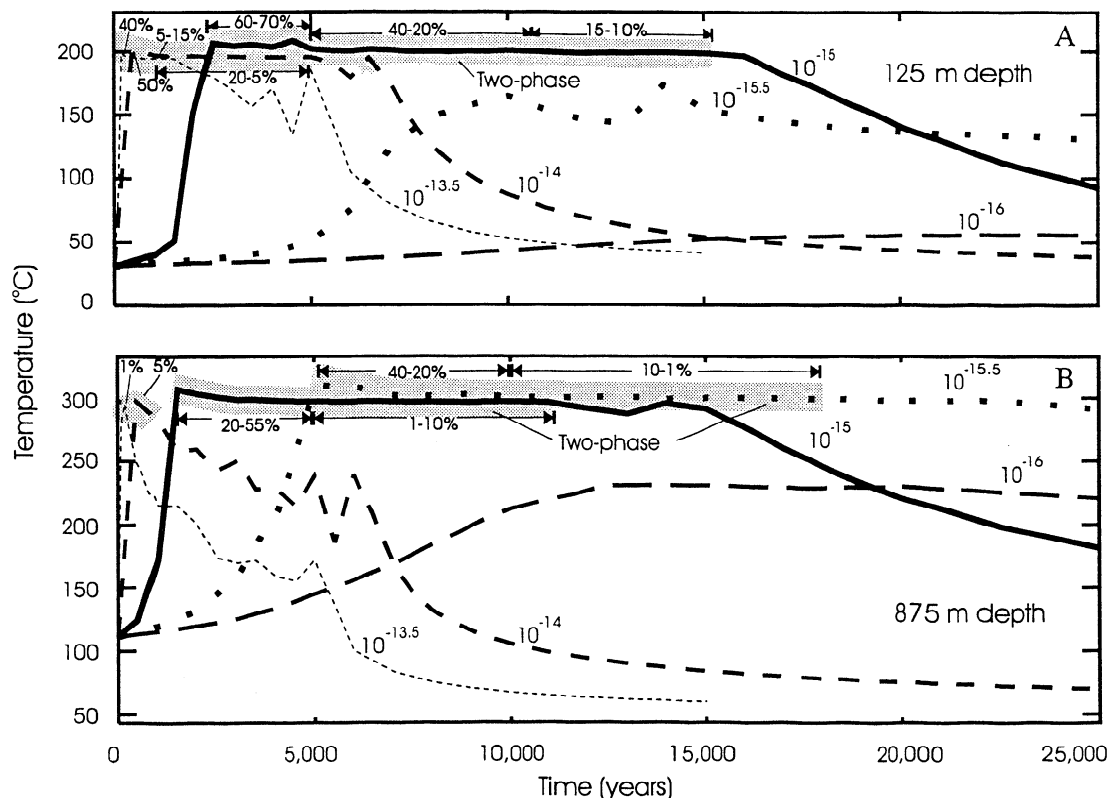


Figure 9. Temperature histories at selected depths above the center of the pluton for conductively preheated host rocks. Volumetric vapor saturation is shown as a percentage.

sions of 2×1 km emplaced at a depth of 5 km into both cool and conductively preheated host rocks. For the preheated simulations, the initial conditions are the 60,000 year solution from an identical model with a host-rock permeability of 10^{-16} m^2 .

Figure 10 shows that hydrothermal systems driven by deep-seated intrusions can develop two-phase conditions even in initially cool host rocks. Norton and Knight [1977, p. 959] stated that plutons emplaced at depths where the fluid pressure exceeds the critical point pressure ($>$ about 2.2 km) do not develop two-phase regions by simple upward transfer of heat. For their choice of pluton permeability (constant at $k = 10^{-18} \text{ m}^2$), boiling would, in fact, be unlikely. However, for pluton permeabilities that are temperature-dependent, with values reaching 10^{-14} m^2 at temperatures below 360°C (Figure 2), near-surface boiling may occur even above deep-seated intrusions. Figure 10 also suggests that it would not be possible to use shallow (<1 km) temperature-depth data to predict the depth of pluton emplacement beneath a permeable hydrothermal system.

Comparing Figure 10 with Figures 6 and 9 indicates that differences between the initially cool and preheated systems are not as great for the deeper (5 km) systems as they are for shallower (2 km) systems. The importance of the initial thermal regime appears to diminish as the depth of pluton emplacement increases. Hydrothermal systems also appear to be more sensitive to the depth of pluton

emplacement than to the initial thermal regime (compare Figure 10b with Figures 6a and 6b).

Effect of Pluton Size

Increasing the dimensions of a pluton adds more heat to a geothermal system and thereby increases its longevity. Larger dimensions can also create interesting variations in the flow pattern. Figure 11 illustrates the evolving hydrothermal system associated with a 2×4 km (2 km half width) pluton emplaced at a depth of 5 km. If the host rock ($k = 10^{-15} \text{ m}^2$) is initially cool, the upwelling plume rises from the outer margin of the pluton, rather than its center, for more than 25,000 years (Figure 11a). This plume is fed by a "normal" hydrothermal convection cell and by a smaller, counter flowing, "Bénard-type" cell that forms directly above the pluton. As the carapace of the pluton freezes and its permeability increases, the flow pattern evolves toward a more typical form (Figure 11b). The rectangular shape of the pluton apparently does not contribute to the Bénard-type convection because simulations for a pluton with stepped corners produced nearly identical results. Norton and Knight [1977] described Bénard-like cells for a batholith-size (54 km width) pluton at 4.5 km depth, and Cathles [1977] suggested that Bénard cells develop above plutons whose total width is comparable to the depth to the top of the pluton. We found that this

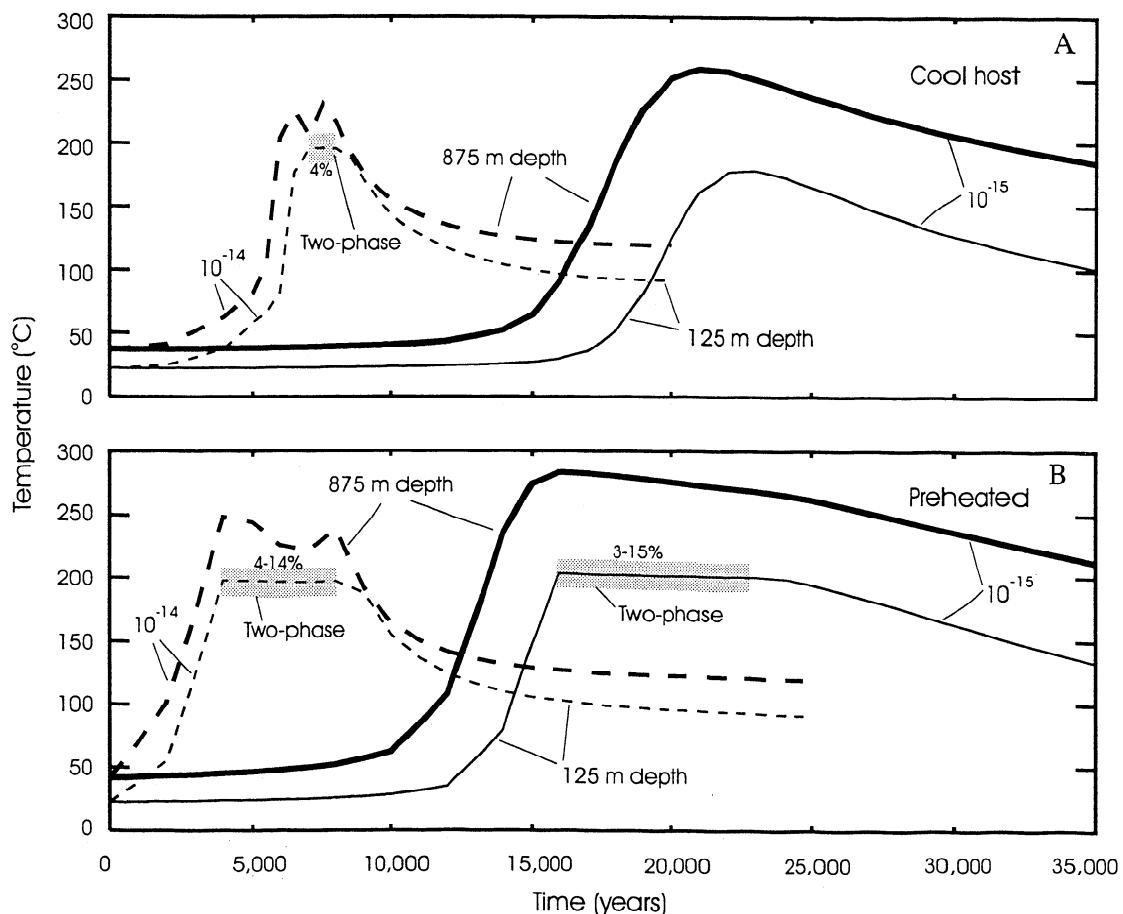


Figure 10. Temperature histories at selected depths above the center of a pluton intruded at 5 km depth into (a) initially cool or (b) preheated host rocks. Volumetric vapor saturation is shown as a percentage.

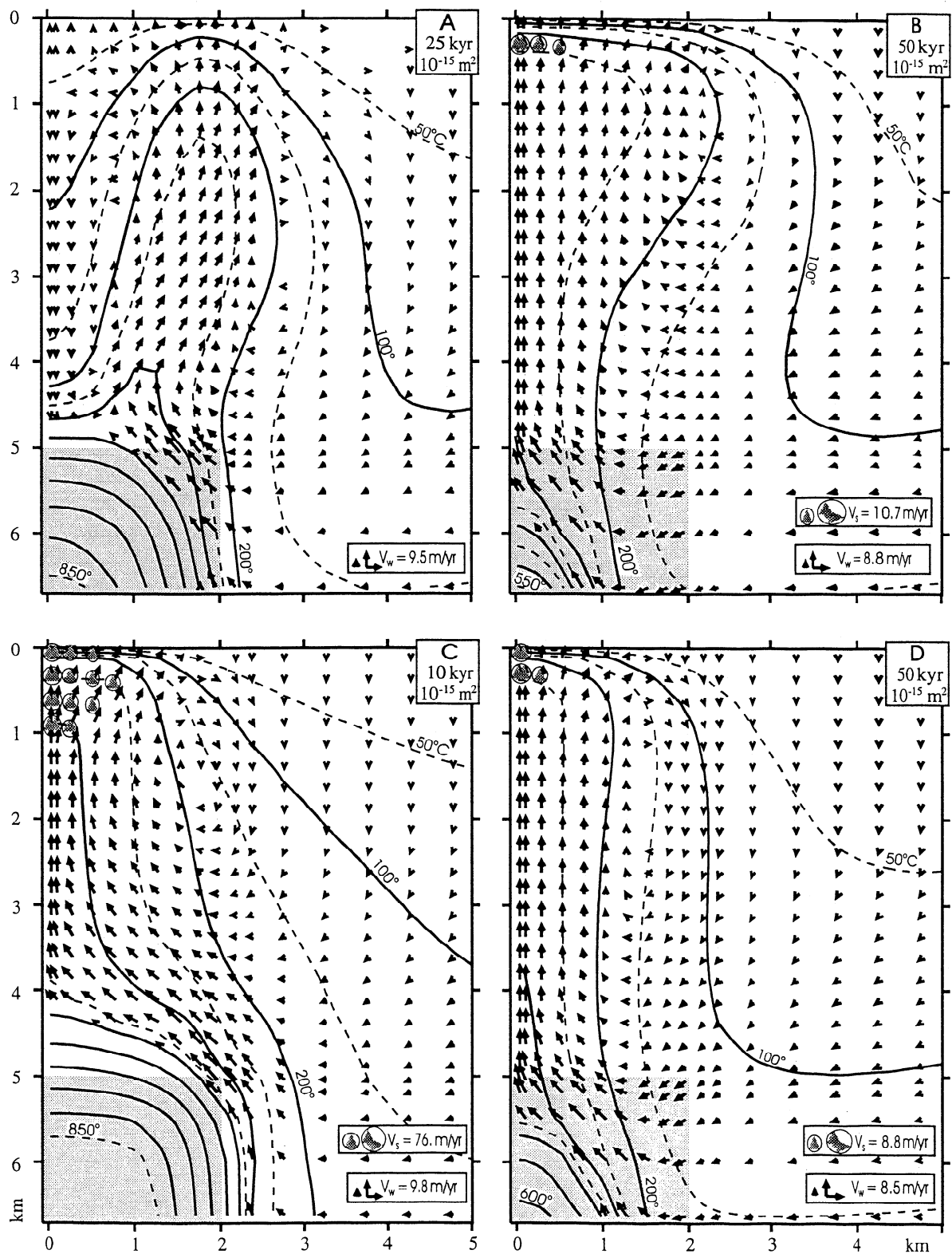


Figure 11. Simulation results for 2 x 4 km (2 km half width) plutons at 5 km depth: (a) results at 25,000 years for initially cool host; (b) results at 50,000 years for initially cool host; (c) results at 10,000 years for preheated host; and (d) results at 50,000 years for preheated host. Permeabilities vary with temperature (Figure 2), and maximum permeability is 10^{-15} m^2 . Flow vectors are as described for Figure 3.

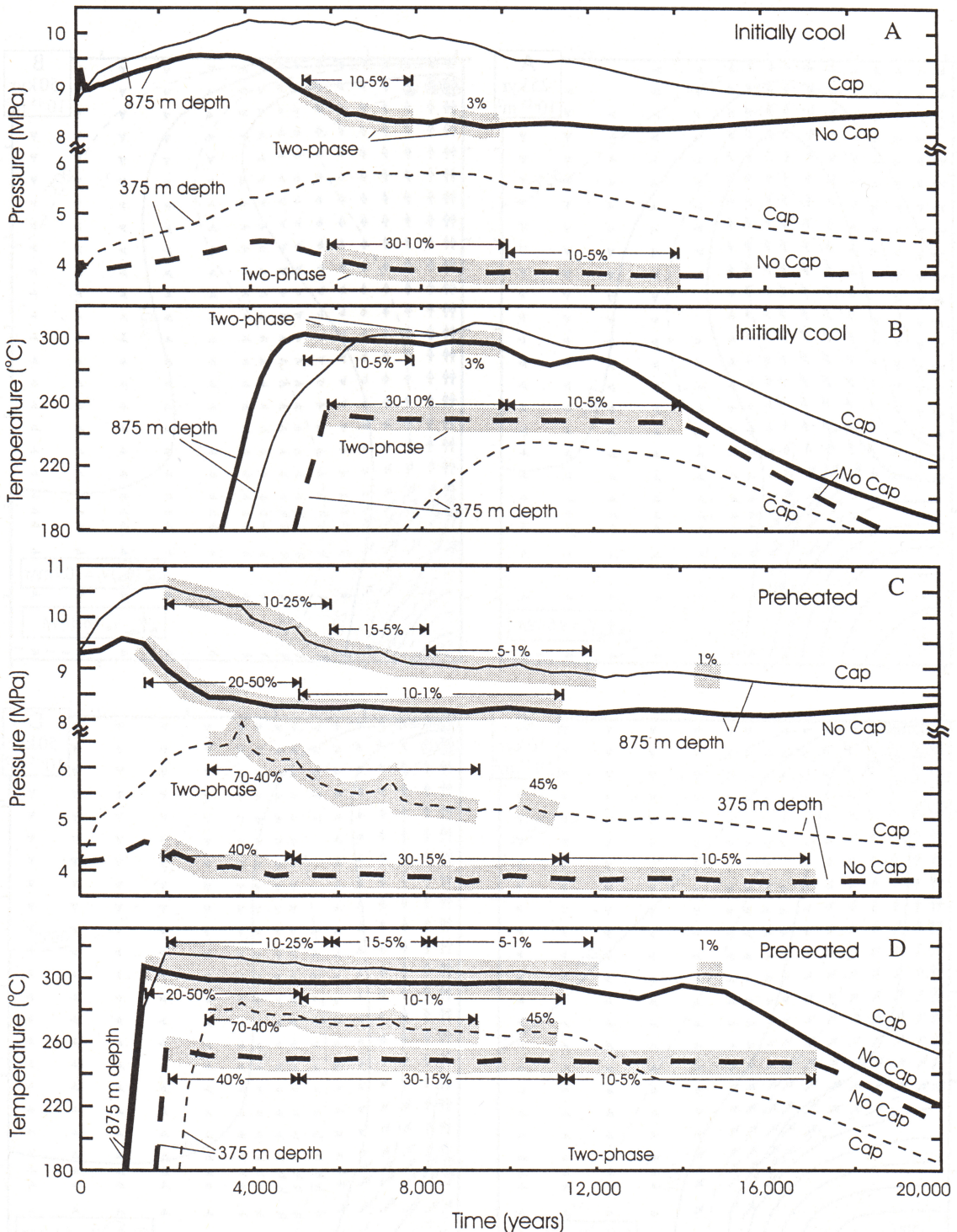


Figure 12. Pressure and temperature histories at selected depths above the center of a cooling pluton in systems with and without caprocks. Permeabilities are 10^{-15} m^2 for the host rock and 10^{-18} m^2 for the caprock. (a) and (b) Results for systems that are initially cool. (c) and (d) Results for systems in which host rocks were conductively preheated by an earlier intrusion. Shaded pattern shows two-phase conditions, with the volumetric percentage of steam indicated.

pattern can also form for narrower plutons (e.g., when the total width is approximately half the depth, as in Figure A2b). However, Bénard-type convection is sensitive to initial thermal conditions. As shown in Figure 11c, a single, large convection cell develops rapidly following intrusion into host rocks preheated by an earlier pluton. By 50,000 years, there is little difference between the flow systems for

the two types of initial conditions (compare Figures 11b and 11d).

Effect of a Caprock

To this point, we have discussed results for systems with homogeneous permeabilities (except for the temperature-

dependent permeability function used above 360°C). Natural systems are, of course, more complex, and one gross feature of many hydrothermal systems is a low-permeability horizon, or caprock, that overlies the more permeable rocks hosting the system. Permeability estimates on the caprocks in the geothermal systems at Wairakei, New Zealand [Mercer and Faust, 1979], Baca, New Mexico [Faust *et al.*, 1984], and Lassen, California [Ingebritsen and Sorey, 1985] and in the Creede epithermal system [Hayba, 1993] suggest that the caprock is 2 to 3 orders of magnitude less permeable than the main hydrothermal system. Here we show results from experiments that incorporate a low-permeability ($k = 10^{-18} \text{ m}^2$) caprock which extends from the land surface to a depth of 250 m and laterally to a distance of 0.6 km from the center of the pluton (Figure 1). Longer caprocks do not significantly alter the simulations.

For intrusions into initially cool host rocks, the caprock tended to suppress the development of two-phase conditions, despite the fact that the capped system produced slightly higher temperatures than the uncapped system. Although the temperature histories for the capped and uncapped systems are similar, especially at 875 m depth (Figure 12b), pressures are significantly greater (by > 1.5 MPa) in the capped systems (Figure 12a). This increased pressure, which inhibits boiling, results from the upwelling plume impinging on the caprock and having to flow laterally before escaping to the surface. The pressure histories also show that fluid pressure at any one point can vary significantly over time. One implication is that pressure estimates based on hydrostatic boiling point depth curves for pure water (ignoring salinity, CO_2 , etc.), which are often made in the context of epithermal deposits, may underestimate pressure by up to 50% because of overpressuring in an upwelling plume beneath a caprock.

In contrast, a caprock significantly increases the maximum steam saturation in systems that have been conductively preheated by an earlier intrusion. In the capped system (Figures 12c and 12d) the volumetric proportion of steam at 375 m depth reaches 70% ($S_w = 0.3$), implying that this region is vapor-dominated because at this saturation liquid water becomes immobile [$k_{rw} = (S_w - 0.3)/0.7$]. These results are consistent with Ingebritsen and Sorey's [1988] work on vapor-dominated hydrothermal systems, which showed that caprocks are an integral aspect of vapor-dominated systems. Systems without caprocks (not shown) that had been preheated either conductively or advectively did not develop vapor-dominated zones.

Effect of Topography

Many intrusions occur in areas with significant topographic relief. In this section, we examine the influence of topography on the evolution of magma-hydrothermal systems with and without caprocks. The topographic relief is centered on the intrusion, which again has a half width of 0.5 km. Figure 13 illustrates the flow patterns for a system with topographic slope of 20% extending laterally from the center of the model (left boundary) to a distance of 2.75 km, at which point the surface becomes flat. The depth to the pluton beneath the highest topographic point is 1.55 km (1 km depth relative to the flat topography). The initial conditions again represent a cool host (20°C/km) at hydrostatic pressures. The host rock has a permeability of 10^{-15}

m^2 , and the caprock shown in Figures 13c and 13d has a permeability of 10^{-18} m^2 .

Without a caprock (Figures 13a and 13b), the position of the interface between the upwelling hydrothermal fluid and the descending shallow groundwater is a strong function of the relative strengths of the topographically and density-driven systems. Shortly after the intrusion of the pluton (Figure 13a), the buoyancy of the hydrothermal fluid is sufficient to force the topographically driven groundwater system to retreat to a depth of about 250 m (relative to the horizontal surface). As the hydrothermal system begins to wane, the interface shifts toward greater depths (e.g., 1 km depth in Figure 13b). The temperature of mixing along the interface between the two systems also changes with time, with the value directly above the pluton increasing from about 150°C at 5000 years to about 260°C at 15,000 years.

For systems with a caprock, the interface between the two flow regimes remains essentially stationary for most of the life of the hydrothermal system (compare Figures 13c and 13d with 13a and 13b). The caprock tends to decouple the topographically driven flow from the underlying hydrothermal system, although leakage through the caprock permits mixing along the interface. Again, temperatures at the interface fluctuate with time, but here they vary only from about 250°C at 5000 years to about 200°C at 15,000 years. The mixing interface is a geochemically favorable environment for precipitating ore minerals, as has been documented for the Creede epithermal system [Plumlee, 1994; Hayba, 1997]. Without a caprock, mineralization would be disseminated as the position of the interface shifted with the waxing and waning of the hydrothermal system. The presence of a caprock may act to stabilize the mixing interface and focus the potential ore-forming environment.

In addition to the hydraulic differences caused by the presence or absence of a caprock, there are also significant differences in the amount and distribution of boiling. In simulations with significant topographic relief, boiling is less prevalent in the uncapped system and occurs, for the most part, at deep levels where temperatures exceed 300°C. In the capped systems, boiling persists to shallower levels and lower temperatures (270° - 290°C). Directly beneath the caprock, steam saturation levels can reach the point at which liquid water becomes immobile (≥ 70 vol % steam). Temperatures are also greater than in the uncapped system, particularly at later times (compare Figures 13b and 13d). By 12,000 years, boiling has ceased in both types of systems.

Magmatic Contributions

Although the HYDROTHERM formulation (equations (1) and (2)) allows for arbitrary sources and sinks, we have not attempted to represent a magmatic fluid contribution. The initial aqueous fluid content of the simulated pluton is about 0.5% by mass (5% porosity with an initial fluid density of about 200 kg/m^3). Because the pluton is initially near lithostatic pressure, some of this fluid is ejected into the hydrothermal system in the early stages of the simulation. However, the fluid content of the region occupied by the pluton later increases to about 1.5% by mass as the fluid density increases to 600 kg/m^3 at 360°C, the temperature at

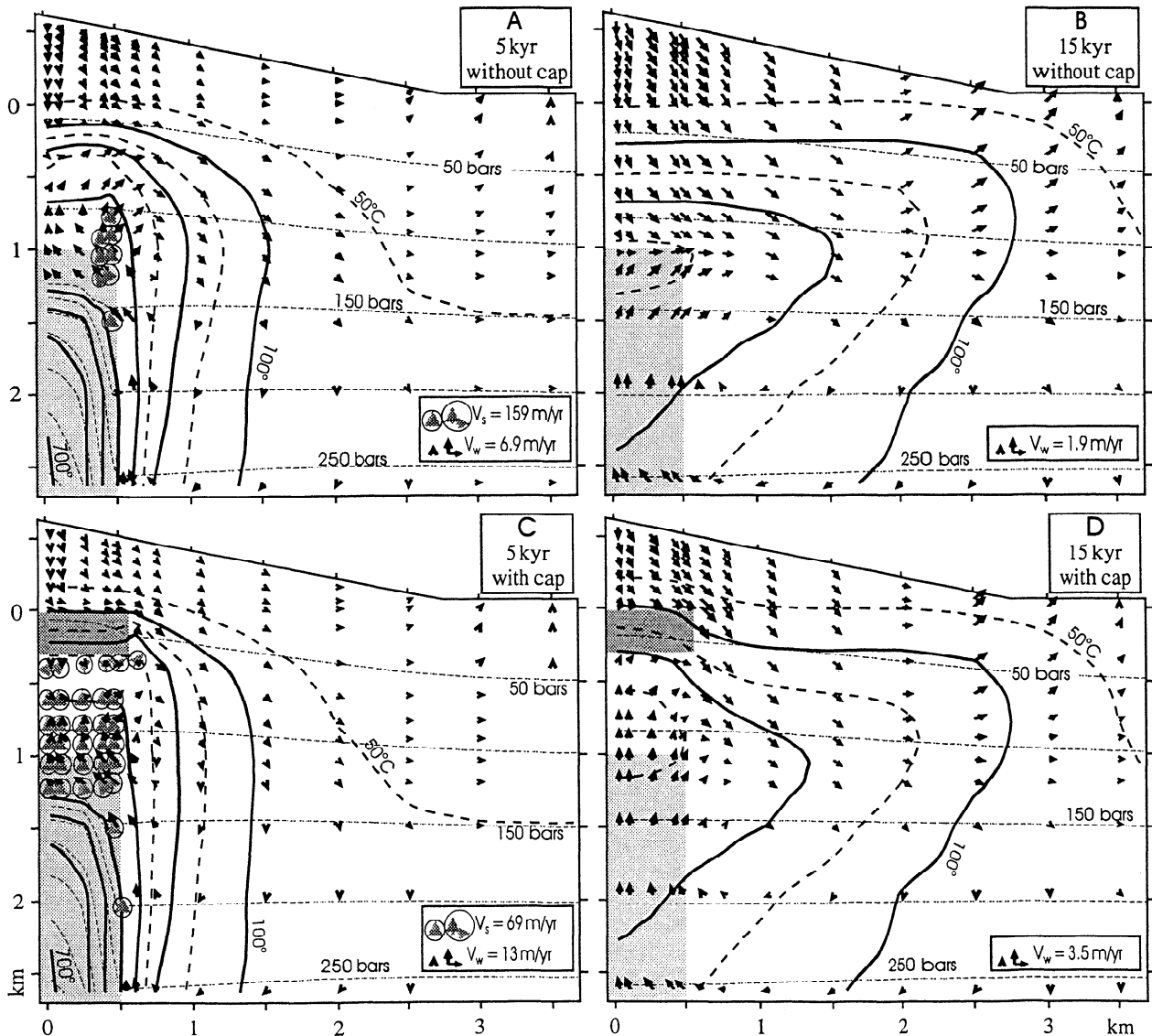


Figure 13. Simulation results for systems with topographic slopes of 20% and the intrusion emplaced at a depth of 1 km relative to the flat topography. Host rock permeability is 10^{-15} m^2 . (a) and (b) No caprock present. (c) and (d) Caprock present (dark shading) with a permeability of 10^{-18} m^2 . The interface between the topographically and density-driven flow systems is defined by converging flow vectors. In the uncapped case, the interface occurs at a depth of about 0.25 km at 5000 years (Figure 13a) and at about 1.0 km at 15,000 years (Figure 13b). In the capped simulation, the interface is located at or just below the caprock. Flow vectors are as described for Figure 3.

which the permeability of the pluton matches that of the host rock.

We have assumed that the magmatic fluid contribution is negligible. This assumption is probably appropriate for the higher permeability simulations ($k \geq 10^{-15} \text{ m}^2$) and at shallow depths, but a significant magmatic component would doubtless affect deeper patterns of fluid flow in the lower-permeability cases where heat transfer is dominated by conduction.

An intrusion can heat roughly its own mass in water [e.g., Norton and Cathles, 1979], so that if the magma releases 4% fluid by mass [Burnham, 1979], the contribution to advection-dominated systems is only about 4%. Most active geothermal systems and epithermal deposits are (were) dominated by advective heat transfer, and stable isotope analyses of epithermal systems typically do not identify

any magmatic signature, although contributions of up to 10% may remain undetected [Rye *et al.*, 1988]. However, magmatic fluids are released mainly in the early part of the cooling history, may be released in bursts, and are concentrated near the top of the magma. Therefore even in the permeability range where advection controls heat transfer ($k \geq 10^{-15} \text{ m}^2$), magmatic fluids may temporarily and locally dominate the hydrologic system.

Hanson's [1995, Figures 5-7] simulations of low-permeability systems ($k = 10^{-16} \text{ m}^2$) show magmatic fluid contributions of 30-90% in the upwelling plume for most of the life of the hydrothermal system. Field evidence from the Philippines [Reyes, 1994, 1995] indicates that only about 10 of more than 400 geothermal wells show considerable magmatic input. These 10 wells do in fact intersect low-permeability horizons (no values reported), as indicated by

rapid pressure drawdown and subsequent discharge of superheated steam. Evidence for a magmatic component includes high-temperature fluids (>330°C) that are often acidic, have very high Cl concentrations (up to 10,000 mg/kg), with $^3\text{He}/^4\text{He}$ ratios > 7 times the ratio in air, high SO_4 contents, and distinctive $\delta^{18}\text{O}$ and δD shifts.

Summary

Our analysis of hydrothermal systems driven by cooling plutons was accomplished using a recently developed, relatively general numerical model for multiphase fluid flow and heat transport in the temperature range of 0°–1200°C. We considered plutons ranging in size from 2 x 1 to 4 x 2 km and emplaced at depths of 2 to 5 km. The slope of the overlying topography ranged from 0 to 20%. Our models treat intrinsic permeability as a temperature-dependent function to simulate the effects of a brittle-ductile transition at about 360°–400°C. Host-rock permeabilities investigated ranged from 10^{-18} m^2 (conduction-dominated systems) to $10^{-13.5} \text{ m}^2$ (advection-dominated systems). We also examined the influence of a caprock and the effects of single versus multiple intrusions. Our results show the following:

1. Host-rock and pluton permeabilities strongly control patterns of fluid circulation and advective heat transfer in hydrothermal systems. The effects of intrusion depth and size and single versus multiple intrusions are secondary.

2. Consistent with the work of *Norton and Knight* [1977], there is a transition from conduction- to advection-dominated heat transport at a permeability of about 10^{-16} m^2 .

3. Consistent with the recent work of *Hanson* [1992, 1995], thermal pressurization of pore fluids in the host rock is a significant driving force for fluid flow for host-rock permeabilities less than or equal to about 10^{-16} m^2 . As fluid sources are depleted, the flow systems in such low-permeability hosts evolve toward the classic buoyancy-driven convection pattern, although heat transfer is dominated by conduction.

4. The hottest hydrothermal systems and most extensive, long-lived, two-phase zones occur in host rocks with permeabilities of about 10^{-15} m^2 . This result appears to be consistent with temperature-permeability relations in natural geothermal reservoirs. Given favorable host-rock permeabilities and initial conditions, two-phase zones can occur above fairly deep intrusions, contrary to the suggestion of *Norton and Knight* [1977].

5. Consistent with the work of *Ingebritsen and Sorey* [1988], vapor-dominated two-phase zones ($k_{rs} \gg k_{rw}$) evolve only when a low-permeability caprock occurs between the intrusion and the land surface. Given the presence of a caprock, vapor-dominated zones can evolve below flat topography in systems "preheated" by previous intrusions or below topographic highs in initially cool systems.

6. For uniform host-rock permeability, the position of the interface between topographically and density-driven flow systems varies substantially as the hydrothermal system waxes and wanes. The presence of a caprock stabilizes the position of the interface thus focusing flow and defining a potential ore-forming environment.

7. Fluid pressures at any point within the upwelling plume can vary substantially with time, ranging from ~1.0 to 1.5 times hydrostatic. Pressures are also highly dependent on the permeability structure, suggesting that assump-

tions concerning boiling point-depth relations may not always be appropriate even when fluid compositions are close to that of pure water.

8. The average magmatic-fluid component in advection-dominated hydrothermal systems (permeability $\geq \sim 10^{-15} \text{ m}^2$) is likely to be less than 10%, consistent with observations on geothermal and epithermal systems but is likely to be much higher in low-permeability host rocks, consistent with calculations by *Hanson* [1995].

Appendix: Comparisons With Early Work

The pioneering work of *Cathles* [1977] and *Norton and Knight* [1977] required several simplifying assumptions. It was also difficult for these researchers to evaluate the accuracy of their solutions because they lacked well-defined sets of benchmark problems, such as those devised somewhat later by the *Stanford Geothermal Workshop* [1980]. Thus we began our experiments by rerunning some of *Cathles'* [1977] and *Norton and Knight's* [1977] original simulations.

Figure A1a shows some of our results for *Cathles'* [1977, Figure 3a] model with a pluton at a depth of 2.75 km and an open upper boundary held at a constant temperature and pressure of 20°C and 1 MPa (10 bars). Other boundary and initial conditions prescribed by *Cathles* include insulating and impermeable sides, a no-fluid-flow basal boundary with a constant heat flux of 63 mW/m², and an initial temperature gradient of 25°C/km. We specified an initial hydrostatic pressure gradient, whereas the stream-function technique employed by *Cathles* [1977] did not require initial conditions for pressure. The dimensions of the pluton are 2.25 km by 0.75 km (half width) with an initial temperature of 700°C. The pluton and the host rocks have identical permeabilities of $2.47 \times 10^{-16} \text{ m}^2$ (0.25 mdarcy), allowing the convecting fluids to extract heat rapidly from the pluton. *Cathles'* models also incorporate a source term of $1.5 \times 10^4 \text{ J}$ per kilogram of intrusive rock to account for exothermic alteration reactions. We included this additional heat by increasing the specific heat of the intrusion from 840 J/(kg K) (as specified by *Cathles* [1977]) to 1140 J/(kg K) for the temperature range 700°–200°C. The specific heat is otherwise 840 J/(kg K). Other relevant matrix properties are porosity (4%), thermal conductivity (2.5 W/(m K)), and rock density (2700 kg/m³).

In general, the agreement between our results (Figure A1a) and those of *Cathles* [1977, Figure 3a] is excellent. Temperature and pressure contours and the location of boiling zones for both models are nearly identical for the five simulation times shown in his Figure 3a. Fluid flow paths also appear similar, but it is difficult to compare accurately our flow vectors with his streamlines. We found that, for this particular simulation, *Cathles* made a reasonable simplifying assumption concerning the lack of two-phase flow (as noted previously, his model treated the fluid as either "all steam" or "all liquid"), because most of the boiling zone in Figure A1a consists of superheated steam rather than a steam/water mixture. However, as we have shown in this paper, two-phase flow is probably much more common than superheated steam in most hydrothermal systems. The abundant superheated steam shown in Figure A1a is a consequence of the relatively high permeability assigned to the pluton, which allows fluids to fully penetrate the 700°C pluton instead of just sweeping heat away from its chilled margins. The lack of a shallow two-

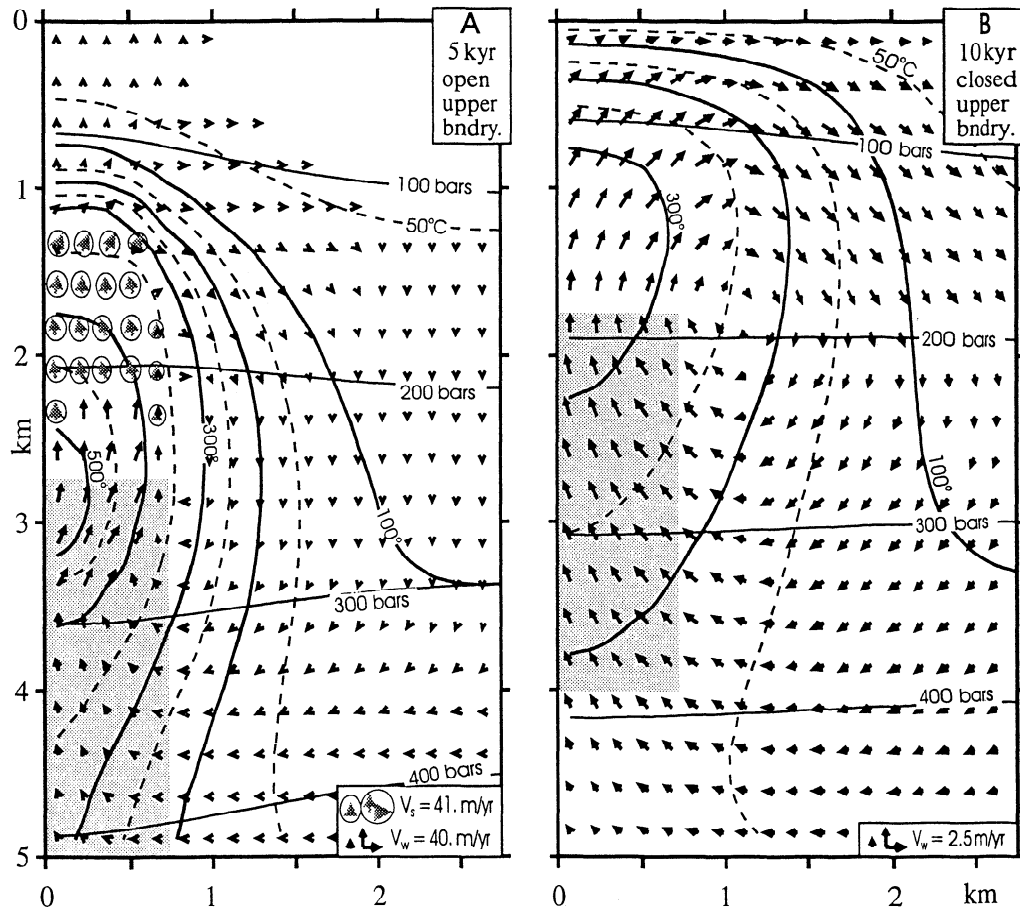


Figure A1. HYDROTHERM simulations of cooling plutons with parameters matching those prescribed by *Cathles* [1977]. (a) Conditions near an intrusion at 2.75 km depth with an open upper boundary at a simulation time of 5000 years (reproducing *Cathles*' Figure 3a). (b) Conditions near an intrusion at 1.75 km depth with an impermeable (closed) upper boundary at a simulation time of 10,000 years (reproducing *Cathles*' Figure 3b). For both models, permeability of host and matrix is $2.47 \times 10^{-16} \text{ m}^2$ (0.25 mDarcy); other parameters are described in text. The right-hand boundary (not shown) is located at a distance of 5 km. Flow vectors are as described for Figure 3.

phase zone in this simulation is due to the relatively low host-rock permeability, which limits advective heat transfer to the near-surface environment.

In the five other simulations presented by *Cathles* [1977], all boundaries, including the top one, are closed to fluid flow. Such boundary conditions are untenable for true variable-density flow simulators that account for the effects of thermal (de-)pressurization. HYDROTHERM simulations with all boundaries closed to flow generate exceedingly high pressures shortly following intrusion emplacement as pore fluids in the host rock expand and then unreasonably low pressures at later times as the pluton cools and the fluids contract. We were able to impose an impermeable upper boundary in our model only by introducing an open boundary along the right-hand side. Under these conditions, our results predict greater pressures for an upwelling plume impinging against a no-flow boundary (Figure A1b) than for flow toward an open upper boundary (Figure A1a), whereas *Cathles*' [1977] models suggest the opposite (see his Figure 12). Our simulations with a no-flow upper boundary also predict considerably less steam production, because of these higher pressures. Our results agree with observations on natural systems, which document higher pressures in geothermal systems with low-

permeability caprocks than in systems without caprocks [e.g., *Grant et al.*, 1982, pp. 27-28]. In a lengthy discussion, *Cathles* [1977] recognized that his method of back-calculating pressure (by integrating Darcy's law and assuming a constant pressure value along the surface) may not be appropriate for closed boundary conditions and that for these conditions the pressure contours should probably reflect an increase in pressure near the surface. Such a change would reduce the extent of boiling predicted by his models but would otherwise have little impact on his results.

Norton and Knight [1977] investigated fluid flow and heat transport around hotter, deeper, larger, and less permeable intrusions than those considered by *Cathles* [1977] and consequently needed to consider longer simulation times (approximately 250,000 years versus 25,000 years). We reproduced *Norton and Knight's* [1977] model P3, which consists of a 4.5 km by 1.35 km (half width) pluton emplaced at a depth of 4.5 km and a temperature of 920°C. The pluton is relatively impermeable (10^{-18} m^2), so that heat must migrate conductively to its margins before entering the more permeable (10^{-15} m^2) country rocks. Like most of *Cathles*' [1977] models, *Norton and Knight's* [1977] model P3 incorporates no-fluid-flow boundaries on all four sides,

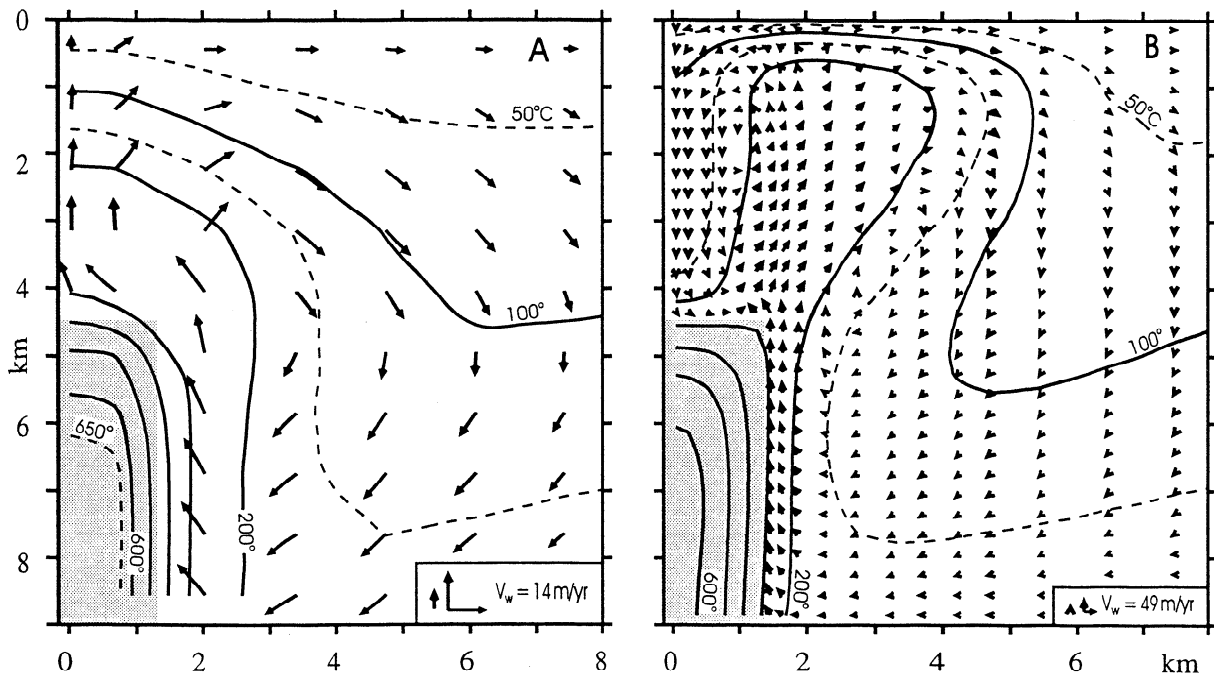


Figure A2. HYDROTHERM simulations of a cooling pluton with (a) model parameters and grid spacing (1,350 m (X) by 900 m (Z)) matching those prescribed by Norton and Knight [1977, model P3] and (b) with identical parameters except grid spacing reduced to approximately 400 m (X) by 300 m (Z). For both models, simulation results are shown at 50,000 years. Permeability is 10^{-18} m² for the pluton and 10^{-15} m² for the country rocks; other parameters are discussed in text. The right-hand boundary (not shown) is located at a distance of 13.5 km. Flow vectors are as described for Figure 3.

and as in the Cathles [1977] comparison (Figure A1b), we maintain a closed top boundary by introducing an open right-hand boundary. Because the right-hand boundary is located at a distance of 13.5 km, this modification has little effect on the temperature solution. We also specified an initial hydrostatic pressure gradient, whereas the stream function-based approach used by Norton and Knight [1977] did not require initial conditions for pressure. Other boundary and initial conditions included a conductive top and an insulating bottom (with no conductive heat input) and an initial temperature gradient of 20°C/km. The other relevant rock-matrix properties are porosity (1%, no value reported by Norton and Knight [1977]), heat capacity (1090 J/(kg K), no value reported by Norton and Knight [1977], value taken from Norton and Cathles [1979]), thermal conductivity (1.2 W/(m K)), and density (2730 kg/m³).

Figure A2a shows our results for Norton and Knight's [1977] model P3 at a simulation time of 50,000 years, using the same coarse grid spacing of 1.35 km (X) by 0.9 km (Z) that they specified. For the first 50,000 years, the temperature regimes predicted by the two models are in reasonably good agreement, and the flow fields indicated by our vectors and their stream functions appear comparable (see their Figure 4). At later times, the results diverge, especially in the higher temperature ($\geq 300^\circ\text{C}$) portions. At 100,000 years, our solutions show maximum temperatures of about 500°C, whereas their solution indicates maximum temperatures of 700°C. At 160,000 years, the difference is 350°C versus 600°C. These large differences may reflect the fact that Norton and Knight's [1977] simulations were not truly transient.

Even more significant differences between our results and those of Norton and Knight [1977] emerge when we use

a finer grid spacing (approximately 400 m in X and 300 m in Z). This more detailed representation of their model P3 predicts two convection cells, rather than a single convection cell (Figure A2b). One of these cells develops to the right of the pluton, while the other is a smaller, secondary Bénard-type cell directly above the pluton. Cathles [1977, Figure 3c], using approximately the same grid spacing, describes a similar pattern of flow around a pluton at 2.75 km depth with a half width of 1.7 km. Norton and Knight [1977, Figure 23] show Bénard-type cells only over batholith-size plutons (27 km half width) at 4.5 km depth.

Acknowledgments. We would like to thank Philip Bethke, Brooks Hanson, Mark Reid, Roger Young, and JGR Associate Editor Robert Lowell for thoughtful and careful reviews. We also appreciate the discussions we had with many colleagues, especially those with Paul Barton, Bruce Christenson, Bruce Gemmill, and Richard Sibson.

References

- Birch, M. U., Groundwater flow systems and thermal regimes near cooling igneous plutons: Influence of surface topography, M.S. thesis, Utah State Univ., Logan, 1989.
- Bischoff, J. L., and K. S. Pitzer, Liquid-vapor relations for the system NaCl-H₂O: Summary of the P-T-x surface from 300° to 500°C, *Am. J. Sci.*, 289, 217-248, 1989.
- Björnsson, G., and G. Bodvarsson, A survey of geothermal reservoir properties, *Geothermics*, 19, 17-27, 1990.
- Brikowski, T., and D. Norton, Influence of magma chamber geometry on hydrothermal activity at mid-ocean ridges, *Earth Planet. Sci. Lett.*, 93, 241-255, 1989.
- Burnham, C. W., Magmas and hydrothermal fluids, in *Geochemistry of Hydrothermal Ore Deposits*, 2nd ed., edited by H. L. Barnes, pp. 71-136, Wiley-Interscience, New York, 1979.
- Cathles, L. M., An analysis of the cooling of intrusives by groundwater convection which includes boiling, *Econ. Geol.*, 72, 804-826, 1977.

- Delaney, P. T., Rapid intrusion of magma into wet rock: Groundwater flow due to pressure increases, *J. Geophys. Res.*, *87*, 7739-7756, 1982.
- Dutrow, B., and D. Norton, Evolution of fluid pressure and fracture propagation during contact metamorphism, *J. Metamorph. Geol.*, *13*, 677-686, 1995.
- Evans, D. G., and J. P. Raffensperger, On the stream function for variable-density groundwater flow, *Water Resour. Res.*, *28*, 2141-2145, 1992.
- Faust, C. R., and J. W. Mercer, Finite-difference model of two-dimensional, single- and two-phase heat transport in a porous medium - Version I, *U.S. Geol. Surv. Open File Rep.*, 77-234, 84 pp., 1977.
- Faust, C. R., and J. W. Mercer, Geothermal reservoir simulation, 1, Mathematical models for liquid- and vapor-dominated hydrothermal systems, *Water Resour. Res.*, *15*, 23-30, 1979.
- Faust, C. R., J. W. Mercer, S. D. Thomas, and W. P. Balleau, Quantitative analysis of existing conditions and production strategies for the Baca geothermal system, New Mexico, *Water Resour. Res.*, *20*, 601-618, 1984.
- Fournier, R. O., Conceptual models of brine evolution in magmatic-hydrothermal systems, in *Volcanism in Hawaii*, edited by R. W. Decker, T. L. Wright, and P. H. Stauffer, *U.S. Geol. Surv. Prof. Pap.*, 1350, pp. 935-946, 1987.
- Fournier, R. O., The transition from hydrostatic to greater than hydrostatic fluid pressure in presently active continental hydrothermal systems in crystalline rock, *Geophys. Res. Lett.*, *18*, 955-958, 1991.
- Furlong, K. P., R. B. Hanson, and J. R. Bowers, Modeling thermal regimes, in *Contact Metamorphism*, edited by D. M. Kerrick, *Rev. Mineral.*, *26*, 437-505, 1991.
- Gerdes, M. L., L. P. Baumgartner, and M. Person, Stochastic permeability models of fluid flow during contact metamorphism, *Geology*, *23*, 945-948, 1995.
- Grant, M. A., I. G. Donaldson, and P. F. Bixley, *Geothermal Reservoir Engineering*, 369 pp., Academic, San Diego, Calif., 1982.
- Haar, L., J. S. Gallagher, and G. S. Kell, *NBS/NRC Steam Tables*, 320 pp., Hemisphere, New York, 1984.
- Haas, J. L., Jr., The effect of salinity on the maximum thermal gradient of a hydrothermal system at hydrostatic pressure, *Econ. Geol.*, *66*, 940-946, 1971.
- Hanson, R. B., Effects of fluid production on fluid flow during regional and contact metamorphism, *J. Metamorph. Geol.*, *10*, 87-97, 1992.
- Hanson, R. B., The hydrodynamics of contact metamorphism, *Geol. Soc. Am. Bull.*, *107*, 595-611, 1995. (Errata, *Geol. Soc. Am. Bull.*, *107*, 1002, 1995.)
- Hanson, R. B., Hydrodynamics of magmatic and meteoric fluids in the vicinity of granitic intrusions, *Trans. R. Soc. Edinburgh Earth Sci.*, *87*, 251-259, 1996.
- Hanson, R. B., and M. D. Barton, Thermal development of low-pressure metamorphic belts: Results from two-dimensional numerical models, *J. Geophys. Res.*, *94*, 10,363-10,377, 1989.
- Hayba, D. O., Numerical hydrologic modeling of the Creede epithermal ore-forming system, Colorado, Ph.D. thesis, Univ. of Ill., Urbana-Champaign, 1993.
- Hayba, D. O., Environment of ore deposition in the Creede Mining District, San Juan Mountains, Colorado, V, Epithermal mineralization from fluid mixing in the OH vein, *Econ. Geol.*, *92*, in press, 1997.
- Hayba, D. O., and S. E. Ingebritsen, The computer model HYDROTHERM, a three-dimensional finite-difference model to simulate ground-water flow and heat transport in the temperature range of 0 to 1,200°C, *U.S. Geol. Surv. Water Resour. Invest. Rep.*, 94-4045, 85 pp., 1994.
- Ingebritsen, S. E., and D. O. Hayba, Fluid flow and heat transport near the critical point of H₂O, *Geophys. Res. Lett.*, *21*, 2199-2203, 1994.
- Ingebritsen, S. E., and M. L. Sorey, A quantitative analysis of the Lassen hydrothermal system, north central California, *Water Resour. Res.*, *21*, 853-868, 1985.
- Ingebritsen, S. E., and M. L. Sorey, Vapor-dominated zones within hydrothermal systems: Evolution and natural state, *J. Geophys. Res.*, *93*, 13,635-13,655, 1988.
- Ingebritsen, S. E., R. H. Mariner, and D. R. Sherrod, Hydrothermal systems of the Cascade Range, north-central Oregon, *U.S. Geol. Surv. Prof. Pap.*, 1044-L, 86 pp., 1994.
- Knapp, R. B., and J. E. Knight, Differential thermal expansion of pore fluids: Fracture propagation and microearthquake production in hot pluton environments, *J. Geophys. Res.*, *82*, 2515-2522, 1977.
- Lowell, R. P., and D. K. Burnell, Mathematical modeling of conductive heat transfer from a freezing, convecting magma chamber to a single-pass hydrothermal system: Implications for seafloor black smokers, *Earth Planet. Sci. Lett.*, *104*, 59-69, 1991.
- Lowell, R. P., P. A. Rona, and R. P. Von Herzen, Seafloor hydrothermal systems, *J. Geophys. Res.*, *100*, 327-352, 1995.
- Manning, C. E., and D. K. Bird, Porosity evolution and fluid flow in the basalts of the Skaergaard magma-hydrothermal system, *Am. J. Sci.*, *291*, 201-257, 1991.
- Mercer, J. W., and C. R. Faust, Geothermal simulation, 3, Application of liquid- and vapor-dominated hydrothermal modeling techniques to Wairakei, New Zealand, *Water Resour. Res.*, *15*, 653-671, 1979.
- Norton, D., Pore fluid pressure near magma chambers, in *The Role of Fluids in Crustal Processes*, edited by J. D. Bredehoeft and D. Norton, pp. 42-49, Nat. Acad. Press, Washington, D. C., 1990.
- Norton, D., and L. M. Cathles, Thermal aspects of ore deposition, in *Geochemistry of Hydrothermal Ore Deposits*, 2nd ed., edited by H. L. Barnes, pp. 611-631, Wiley-Interscience, New York, 1979.
- Norton, D., and J. E. Knight, Transport phenomena in hydrothermal systems: Cooling plutons, *Am. J. Sci.*, *277*, 937-981, 1977.
- Norton, D., and H. P. Taylor Jr., Quantitative simulation of the hydrothermal systems of crystallizing magmas on the basis of transport theory and oxygen isotope data: Analysis of the Skaergaard intrusion, *J. Petrol.*, *20*, 421-486, 1979.
- Parmentier, E. M., Numerical experiments on ¹⁸O depletion in igneous intrusions cooling by groundwater convection, *J. Geophys. Res.*, *86*, 7131-7144, 1981.
- Plumlee, G. S., Fluid chemistry evolution and mineral deposition in the main-stage Creede epithermal system, *Econ. Geol.*, *89*, 1860-1882, 1994.
- Pruess, K., TOUGH2 - A general-purpose numerical simulator for multiphase fluid and heat flow, *Rep. LBL-29400*, 102 pp., Lawrence Berkeley Laboratory, Berkeley, Calif., 1991.
- Reyes, A. G., Petrological and geochemical characteristics of magmatic-hydrothermal systems in the Philippines, in *Extended Abstracts of Workshop on Deep-Seated and Magma-Ambient Geothermal Systems*, pp. 121-125, New Energy and Ind. Technol. Dev. Organ., Tsukuba, Japan, 1994.
- Reyes, A. G., Geothermal systems in New Zealand and the Philippines - Why are they so different?, in *Proceedings of the 1995 PACRIM Congress, Publ. Ser.*, vol. 9/95, edited by J. L. Mauk and J. D. St. George, pp. 485-490, Australas. Inst. Min. and Metal., Carlton, Victoria, Australia, 1995.
- Rye, R. O., G. S. Plumlee, P. M. Bethke, and P. B. Barton, Stable isotope geochemistry of the Creede, Colorado, hydrothermal system, *U.S. Geol. Surv. Open File Rep.*, 88-356, 40 pp., 1988.
- Sammel, E. A., S. E. Ingebritsen, and R. H. Mariner, The hydrothermal system at Newberry volcano, Oregon, *J. Geophys. Res.*, *93*, 10,149-10,162, 1988.
- Sengers, J. V., and J. T. R. Watson, Improved international formulation for the viscosity and thermal conductivity of water substance, *J. Phys. Chem. Ref. Data*, *15*, 1291-1314, 1986.
- Stanford Geothermal Workshop, Proceedings of the special panel on geothermal model intercomparison study, *Dep. of Energy Rep. DOE/SF/11459-1*, 120 pp., Stanford Univ., Palo Alto, Calif., 1980.
- Taylor, H. P., Jr., Oxygen and hydrogen isotope constraints on the deep circulation of meteoric waters, in *The Role of Fluids in Crustal Processes*, edited by J. D. Bredehoeft and D. Norton, pp. 72-95, Nat. Acad. Press, Washington, D. C., 1990.
- Takasaki, K. J., Ground-water occurrence in Kilauea volcano and adjacent parts of Mauna Loa volcano, *U.S. Geol. Surv. Open File Rep.* 93-82, 28 pp., 1993.

D. O. Hayba, U.S. Geological Survey, Mail Stop 956, National Center, Reston, VA 20192 (email: dhayba@usgs.gov)

S. E. Ingebritsen, U.S. Geological Survey, Mail Stop 439, 345 Middlefield Rd., Menlo Park, CA 94025 (email: seingebr@usgs.gov)

(Received September 25, 1996; revised January 15, 1997; accepted February 18, 1997.)